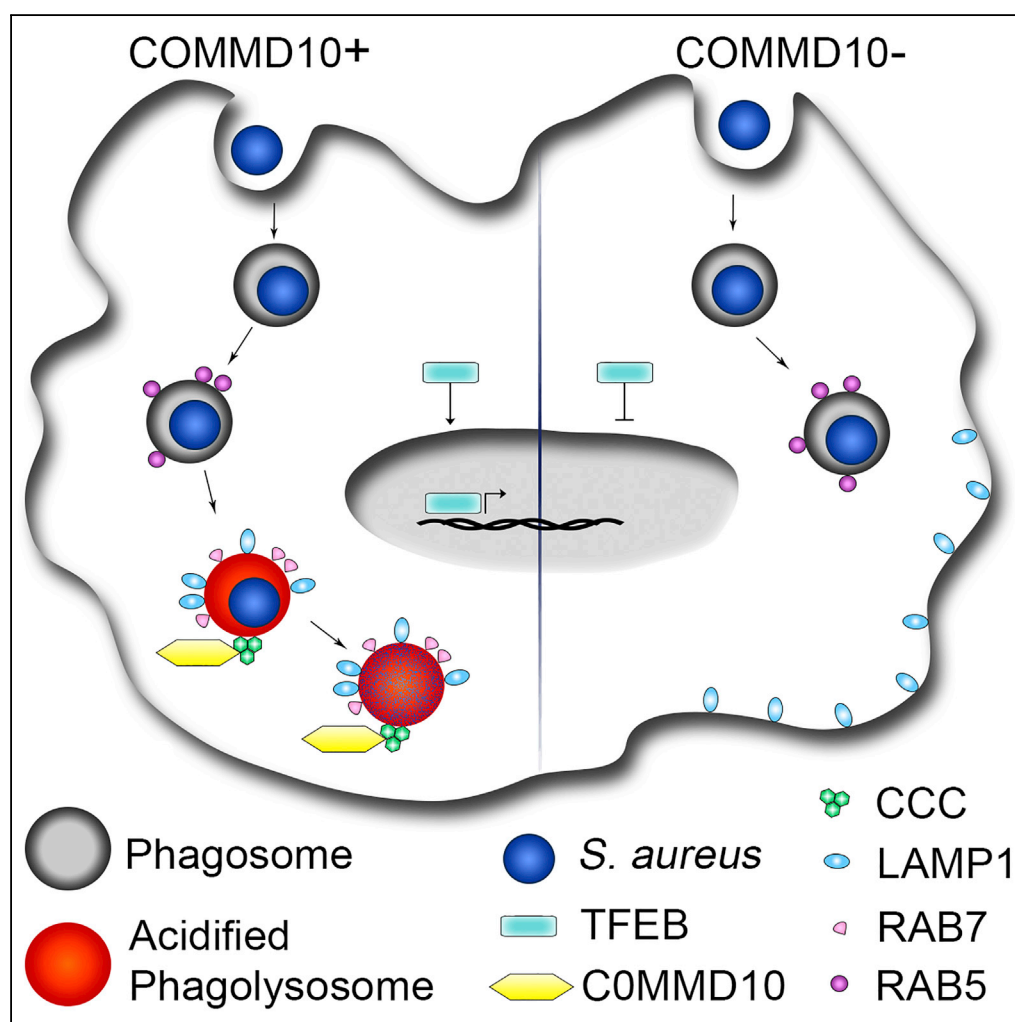


## Article

COMMD10-Guided Phagolysosomal Maturation Promotes Clearance of *Staphylococcus aureus* in Macrophages

Shani Ben Shlomo,  
Odelia  
Mouhadeb, Keren  
Cohen, Chen  
Varol, Nathan  
Gluck

chenv@tlvmc.gov.il (C.V.)  
nathang@tlvmc.gov.il (N.G.)

**HIGHLIGHTS**

COMMD10 facilitates  
timely clearance of  
*S. aureus* by liver Kupffer  
cells

COMMD10 drives  
transcription program of  
lysosome biogenesis in  
infected macrophages

COMMD10 drives  
phagolysosomal  
maturation and  
acidification in infected  
macrophages

## Article

# COMMD10-Guided Phagolysosomal Maturation Promotes Clearance of *Staphylococcus aureus* in Macrophages

Shani Ben Shlomo,<sup>1,3</sup> Odelia Mouhadeb,<sup>1,2,3</sup> Keren Cohen,<sup>1,2</sup> Chen Varol,<sup>1,2,4,\*</sup> and Nathan Gluck<sup>1,4,5,\*</sup>**SUMMARY**

*Staphylococcus aureus* is a major cause of infectious disease. Liver Kupffer cells (KCs) are responsible for sequestering and destroying *S. aureus* through the phagolysosomal pathway. Proteins belonging to the COMMD family emerge as key intracellular regulators of protein trafficking, but the role of COMMD10 in macrophage-mediated *S. aureus* eradication is unknown. Here we report that COMMD10 in macrophages was necessary for its timely elimination, as demonstrated with two different *S. aureus* subspecies. *In vivo*, COMMD10-deficient liver KCs exhibited impaired clearance of systemic *S. aureus* infection. *S. aureus*-infected COMMD10-deficient macrophages exhibited impaired activation of the transcription factor EB, resulting in reduced lysosomal biogenesis. Moreover, *S. aureus*-initiated phagolysosomal maturation and function were significantly attenuated in COMMD10-deficient macrophages. Finally, expression of COMMD/CCDC22/CCDC93 complex, linked to phagolysosomal maturation, was reduced by COMMD10 deficiency. Collectively, these results support an important role for COMMD10 in instructing macrophage phagolysosomal biogenesis and maturation during *S. aureus* infection.

**INTRODUCTION**

Macrophages are immune cells of the myeloid lineage that are strategically positioned in all organs of the body, where they perform tissue-specific functions. A generic macrophage function is to act as immune sentinels in the frontline of tissue defense against infectious invaders, especially at barrier organs, which represent putative entry and colonization sites for pathogens (Varol et al., 2015). Macrophages are armed with a large repertoire of pattern recognition receptors that determine their immunologic and homeostatic potential (Taylor et al., 2005). They are keen in internalizing and destroying invading organisms by trapping them in phagosomes. These structures undergo a sequence of transformations termed phagolysosomal maturation, whereby phagosomal membrane and contents acquire a wide arsenal of microbicidal and lytic features through a strictly choreographed sequence of fusion and fission events with trans-Golgi transport vesicles, endosomes, lysosomes, and autophagosomes (Fair and Grinstein, 2012; Flannagan et al., 2009).

*Staphylococcus aureus* is a highly adaptable human pathogen causing significant morbidity and mortality due to both community- and hospital-acquired infections (Lowy, 1998; Magill et al., 2014). The pathogenicity of *S. aureus* is enhanced by its capacity to cause bacteremia and by the emergence of high-level antimicrobial resistance strains, such as methicillin-resistant *S. aureus*. Macrophages initiate intracellular microbicidal mechanisms to rapidly kill *S. aureus* after ingestion. However, when exposed to large inocula of *S. aureus*, they become progressively exhausted, leading to incomplete phagolysosomal maturation and acidification and to a persisting pool of viable intracellular bacteria (Flannagan et al., 2016; Jubrail et al., 2016). Enabled by a variety of virulence factors and an intricate network of regulators, a few *S. aureus* survive within phagocytes and disseminate to non-phagocytic cells leading to tissue destruction and persistence of infection (Horn et al., 2018; Pollitt et al., 2018; Strobel et al., 2016). In particular, liver intravascular Kupffer cells (KCs) are primarily responsible for the initial sequestration and killing of circulating *S. aureus* within minutes. However, a minority of the staphylococci can sometimes overcome KC antimicrobial defenses, survive and proliferate within this intracellular niche, and ultimately escape to colonize other tissues (Pollitt et al., 2018; Surewaard et al., 2016).

Macrophage phagocytic activities must be tightly regulated to allow for rapid escalation in case of *S. aureus* invasion. Therefore it is essential to define the regulatory pathways that shape the macrophage innate immune responses to *S. aureus* infection. The COMMD family includes 10 evolutionarily conserved proteins

<sup>1</sup>The Research Center for Digestive Tract and Liver Diseases, Tel-Aviv Sourasky Medical Center and Sackler School of Medicine, Tel-Aviv University, 6 Weizmann St, Tel-Aviv 64239, Israel

<sup>2</sup>Department of Clinical Microbiology and Immunology, Sackler School of Medicine, Tel-Aviv University, Tel-Aviv 69978, Israel

<sup>3</sup>These authors contributed equally

<sup>4</sup>These authors contributed equally

<sup>5</sup>Lead Contact

\*Correspondence: chenv@tlvmc.gov.il (C.V.), nathang@tlvmc.gov.il (N.G.)  
<https://doi.org/10.1016/j.isci.2019.03.024>



that share a highly conserved and unique motif in their carboxyl terminus termed *copper metabolism gene MURR1 domain* (COMMD), which functions as an interface for protein-protein interactions. Several functions have been linked to members of the COMMD protein family, which can be broadly grouped into two categories: transcription factor regulation and regulation of intracellular cargo-specific trafficking via interaction with components of the endolysosomal pathway. Previous work in human cell lines has established that all COMMD proteins are negative regulators of the nuclear factor (NF)- $\kappa$ B pathway (Burstein et al., 2005; Maine et al., 2007; Mouhadeb et al., 2018). This was further corroborated in transgenic mouse systems, in which targeting of COMMD1 or COMMD10 deficiencies to myeloid cells resulted in increased NF- $\kappa$ B activation and subsequent exacerbation of lipopolysaccharide (LPS)-induced sepsis and dextran sodium sulfate-induced colitis (Li et al., 2014; Mouhadeb et al., 2018). Additional transcriptional programs that are controlled by COMMD1 include hypoxia-inducible factor (HIF) and E2F1 (Muller et al., 2009; Murata et al., 2017; van de Sluis et al., 2010). Emerging findings also indicate that COMMD proteins play important roles in tuning intracellular signaling and protein trafficking pathways that are highly relevant to macrophage bactericidal activity. In particular, studies in human cells revealed that COMMD proteins are essential components of the COMMD/CCDC22/CCDC93 (CCC) protein complex (Li et al., 2015; Phillips-Krawczak et al., 2015; Starokadomskyy et al., 2013). This complex interacts with the Wiscott-Aldrich and Scar Homolog (WASH) complex (Bartuzi et al., 2016; Phillips-Krawczak et al., 2015), which is intimately linked to bacterial phagocytosis (Buckley et al., 2016) and subsequent lysosomal maturation (King et al., 2013). We have recently shown in human embryonic kidney (HEK) cells that COMMD10 binds the CCDC22 component of the CCC complex (Starokadomskyy et al., 2013). Moreover, COMMD10 has been identified by proteomics to be associated with phagosomes in murine macrophages (Dill et al., 2015). Both these features of COMMD10 prompted us to study its possible involvement in mediating macrophage immune response to *S. aureus* infection.

Here we report the establishment of transgenic COMMD10 conditional knockout mice allowing the targeting of its deficiency to myeloid cells and specifically macrophages. We show that COMMD10 in macrophages propagates phagolysosome maturation and function to facilitate adequate killing of *S. aureus* bacteria.

## RESULTS

### COMMD10 Deficiency Impairs KC-Governed Elimination of *S. aureus* in the Liver

Liver-resident macrophages, namely, KCs, are the key cell population responsible for eliminating *S. aureus* from the circulation (Surewaard et al., 2016). Hence, we first examined *in vivo* whether *S. aureus* handling is influenced by COMMD10 deficiency in KCs. The study of COMMD10 immunoregulation in macrophages has been hampered by embryonic lethality of COMMD10 knockout mice. To overcome this obstacle, we generated transgenic mice that allow specific targeting of COMMD10 deficiency to macrophages by crossing *Commd10<sup>fl/fl</sup>* mice (Mouhadeb et al., 2018) with *Cx3cr1<sup>cre</sup>* mice (Yona et al., 2013). In these mice, cre-driven recombination (and the ensuing COMMD10 deficiency) is largely restricted to tissue-resident macrophages, and specifically in the liver to KCs (Yona et al., 2013), as well as to recently defined CX<sub>3</sub>CR1<sup>+</sup> liver capsular macrophages (LCMs) (Sierro et al., 2017) and a subset of dendritic cells (David et al., 2016). The resulting *Cx3cr1<sup>ΔCommd10</sup>* mice exhibited normal birth rate and life expectancy (data not shown). Data mining into gene expression databases of sorted steady-state KCs (Zigmond et al., 2014) and LCMs (Sierro et al., 2017) confirmed the expression of *Commd10* in both subsets (Figure S1A). *Cx3cr1<sup>ΔCommd10</sup>* mice infected with GFP-tagged SH1000 strain of *S. aureus* showed a higher burden of bacteria in the blood (Figure 1A) and liver (Figure 1B) 3 h post intravenous inoculation. The increased bacteremia persisted at 24 h post infection (Figure 1C). We next focused on KCs in light of their key role in handling of circulating *S. aureus* infection. Despite similar abundance of KCs at baseline (Figure 1D), KC numbers were decreased in *Cx3cr1<sup>ΔCommd10</sup>* mice following infection (Figure 1E), and accordingly, the KC fraction out of liver CD45<sup>+</sup> leukocytes was lower at 3 and 24 h (Figures 1F and 1G). Looking at the bacterial signal from the remaining KCs, a higher mean fluorescent intensity (MFI) of GFP-tagged *S. aureus* was observed in infected *Cx3cr1<sup>ΔCommd10</sup>* versus *Commd10<sup>fl/fl</sup>* KCs (Figure 1H).

*Cx3cr1<sup>ΔCommd10</sup>* mice infected for 24 h with the untagged Rosenbach strain of *S. aureus* exhibited increased hepatic damage, as manifested by more abundant and extended subcapsular and parenchymal necrotic lesions (Figures S1B and S1C) and increased serum levels of the liver enzymes alanine and aspartate aminotransferases (Figure S1D). Increased bacteremia (Figure S1E), weight loss (Figure S1F), and serum creatine phosphokinase

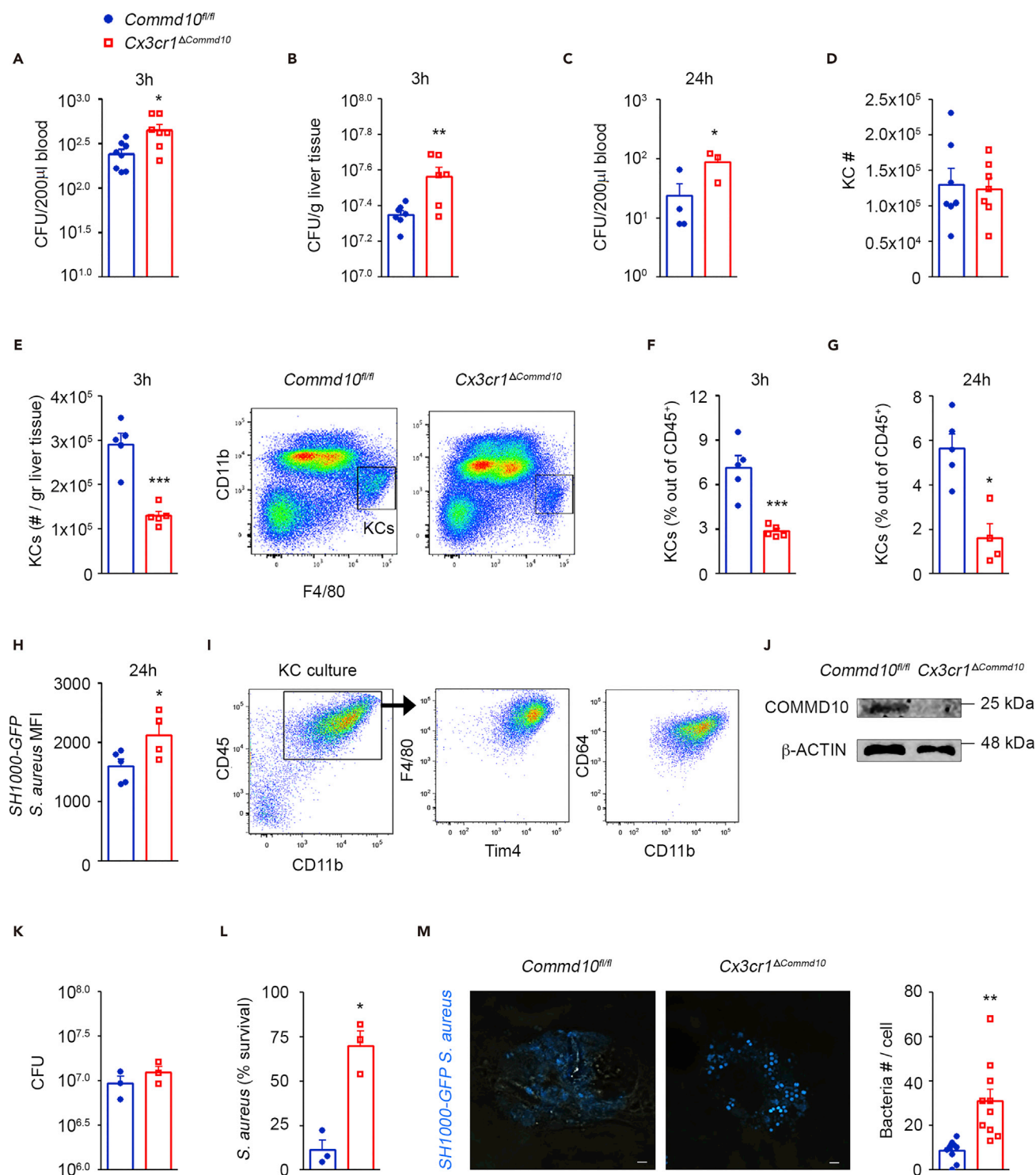


**Figure 1. Impaired Clearance of *S. aureus* Infection by COMMD10-Deficient KCs**

(A–H) *Commd10<sup>fl/fl</sup>* (blue, closed circles) or *Cx3Cr1<sup>ΔCommd10</sup>* (red, open squares) mice were intravenously injected with SH1000-GFP *S. aureus* ( $5 \times 10^7$  CFU per animal). (A and C) Blood and (B) liver specimens were extracted at 3 h ( $n \geq 7$ ) and 24 h ( $n \geq 3$ ) following *S. aureus* injection. Colony-forming units (CFU) were determined per 0.2 mL of blood (A and C) or normalized to liver tissue mass (B). (D) Flow cytometry-based assessment of liver-resident KC numbers at steady state ( $n = 7$  from a single experiment). (E) Assessment of liver-resident KC numbers at 3 h ( $n = 5$ ). Right panel, flow cytometry gating strategy of KCs. (F and G) Assessment of KC fraction out of total CD45<sup>+</sup> immune cells at 3 h (F) and at 24 h (G) following *S. aureus* injection ( $n = 5$ ). (H) SH1000-GFP *S. aureus* signal intensity in KCs as depicted by MFI ( $n = 5$ ).

**Figure 1. Continued**

(I–M) Liver KCs isolated from *Commd10<sup>fl/fl</sup>* and *Cx3cr1<sup>dCommd10</sup>* mice were infected with *SH1000-GFP* or untagged *S. aureus* at MOI = 5 ( $n \geq 3$  mice). (I) Flow cytometry images showing isolated KC purity. (J) Immunoblots demonstrating the expression of COMMD10.  $\beta$ -Actin was used as a control ( $n = 2$  biological repeats, each composed of a pool from four mice). (K) CFU of lysed KCs at 30 min following *S. aureus* injection. (L) Survival of *S. aureus* in KCs at 2 h following injection assessed by gentamycin protection assay. (M) Confocal microscopic images showing accumulation of *SH1000-GFP S. aureus* (cyan) at 1 h post infection. Magnification,  $\times 40$ ; scale bar, 2  $\mu$ M ( $n \geq 10$  imaged cells per group [ $n \geq 3$ ]). Right panel: quantification of bacteria in confocal imaging. Data in (A), (B), (D–F), and (M) were analyzed by unpaired, two-tailed t test, and data in (C), (G), (H), (K), and (L) were analyzed by non-parametric Mann-Whitney test, comparing each time between *Commd10<sup>fl/fl</sup>* and *Cx3cr1<sup>dCommd10</sup>* groups. Results are presented as mean  $\pm$  SEM with significance: \* $p < 0.05$ , \*\* $p < 0.01$ , \*\*\* $p < 0.001$

levels (Figure S1G) further supported aggravated systemic disease in the *Cx3cr1<sup>dCommd10</sup>* mice. Similar to infection with SH1000 *S. aureus* strain, there were significantly reduced numbers and fraction of KCs in the *Cx3cr1<sup>dCommd10</sup>* livers, concomitantly with a dramatic increase in the infiltration of Ly6C<sup>hi</sup> monocytes, but not of neutrophils (Figures S1H and S1I). The prevalence of late apoptotic PI<sup>+</sup>AnnexinV<sup>+</sup> KCs was increased as well in the *Cx3cr1<sup>dCommd10</sup>* livers (Figure S1J). Together, these findings suggest increased death of COMMD10-deficient KCs associated with an increased bacterial burden.

To directly test for a role of COMMD10 in KC bacterial handling, we next challenged primary KC isolated from *Cx3cr1<sup>dCommd10</sup>* versus *Commd10<sup>fl/fl</sup>* mice with *S. aureus*. KC enrichment was confirmed by combined expression of the lineage-specific markers F4/80, Tim4, and CD64 (FcyR) (Figure 1I), and efficient deficiency of COMMD10 protein was evident in *Cx3cr1<sup>dCommd10</sup>* KC (Figure 1J). *Cx3cr1<sup>dCommd10</sup>* KCs exhibited similar internalization of *S. aureus* at 30 min post infection (Figure 1K). However, their clearance of *S. aureus* was dramatically impaired at 2 h following infection (Figure 1L). Confocal microscopy further validated the increased accumulation of GFP-tagged *S. aureus* in the COMMD10-deficient KCs (Figure 1M). Together, these findings show that COMMD10 in KC plays an important role in the liver barrier function against invading *S. aureus*.

**COMMD10 Is Essential for Timely Clearance of *S. aureus* by Macrophages**

Given the scarcity of cells achieved in KC cultures, we next chose bone marrow (BM)-derived macrophages (BMDM) as a prototype population of primary macrophages for our studies. BMDM were generated from *LysM<sup>dCommd10</sup>* mice in which COMMD10 deficiency has been targeted to myeloid cells by crossing *Lyz2<sup>cre</sup>* mice with *Commd10<sup>fl/fl</sup>* mice. Efficient deficiency of COMMD10 protein, but not of COMMD1, was evident in *LysM<sup>dCommd10</sup>* BMDM infected with *S. aureus* (Figure 2A). At the transcription level, the *LysM<sup>dCommd10</sup>* BMDM exhibited specific reduction in *Commd10* expression, whereas the expression of all other *Commd* genes was not significantly altered (Figure 2B). BMDM from *Commd10<sup>fl/fl</sup>* or *LysM<sup>dCommd10</sup>* mice were infected with *S. aureus* or *Staphylococcus xylosum* for 30 min, and their intracellular levels were then evaluated at distinct time points using the gentamycin protection assay followed by seeding and colony-forming unit (CFU) counting. Similarly to COMMD10-deficient KCs (Figures 1L and 1M), *LysM<sup>dCommd10</sup>* BMDM exhibited significantly delayed clearance of *S. aureus* over time as manifested by increased CFU at 4, 6, and 24 h following infection (Figure 2C). Comparable results were obtained following *S. xylosum* infection showing impaired clearance at 2, 4, and 6 h following infection (Figure 2D). These results were further corroborated by flow cytometry revealing increased MFI at 2 h following infection with GFP-tagged *S. aureus* (Figure 2E). Confocal microscopy further demonstrated increased accumulation of GFP-tagged *S. aureus* bacteria in phagosomal compartments of COMMD10-deficient macrophages at 4 h following infection (Figure 2F). In BM-derived neutrophils, COMMD10 deficiency had no clear effect on the handling of *S. xylosum* (Figure 2G), suggesting that COMMD10 does not play a role in neutrophil-mediated bactericidal activity against staphylococci. Collectively, these findings highlight that COMMD10 is required for the timely elimination of intracellular *S. aureus* infection in macrophages.

**COMMD10 Does Not Play a Role in Macrophage-Mediated Internalization of *S. aureus***

Phagocytosis is a hallmark of anti-bacterial host defense. The attenuated clearance of *S. aureus* in COMMD10-deficient macrophages *in vivo* (Figure 1) and *in vitro* (Figure 2) may be the outcome of its impaired internalization. To study the involvement of COMMD10 in macrophage-governed phagocytosis of staphylococci, BMDM from *Commd10<sup>fl/fl</sup>* or *LysM<sup>dCommd10</sup>* mice were infected with *S. aureus* or *S. xylosum* for 30 min, and their intracellular levels were immediately evaluated using the gentamycin protection assay followed by seeding and CFU counting. COMMD10-deficient and COMMD10-proficient BMDM exhibited similar intracellular bacterial counts of both *S. aureus* and *S. xylosum* (Figure 3A). In addition, flow cytometry analysis revealed that COMMD10 deficiency had no effect on the MFI of internalized

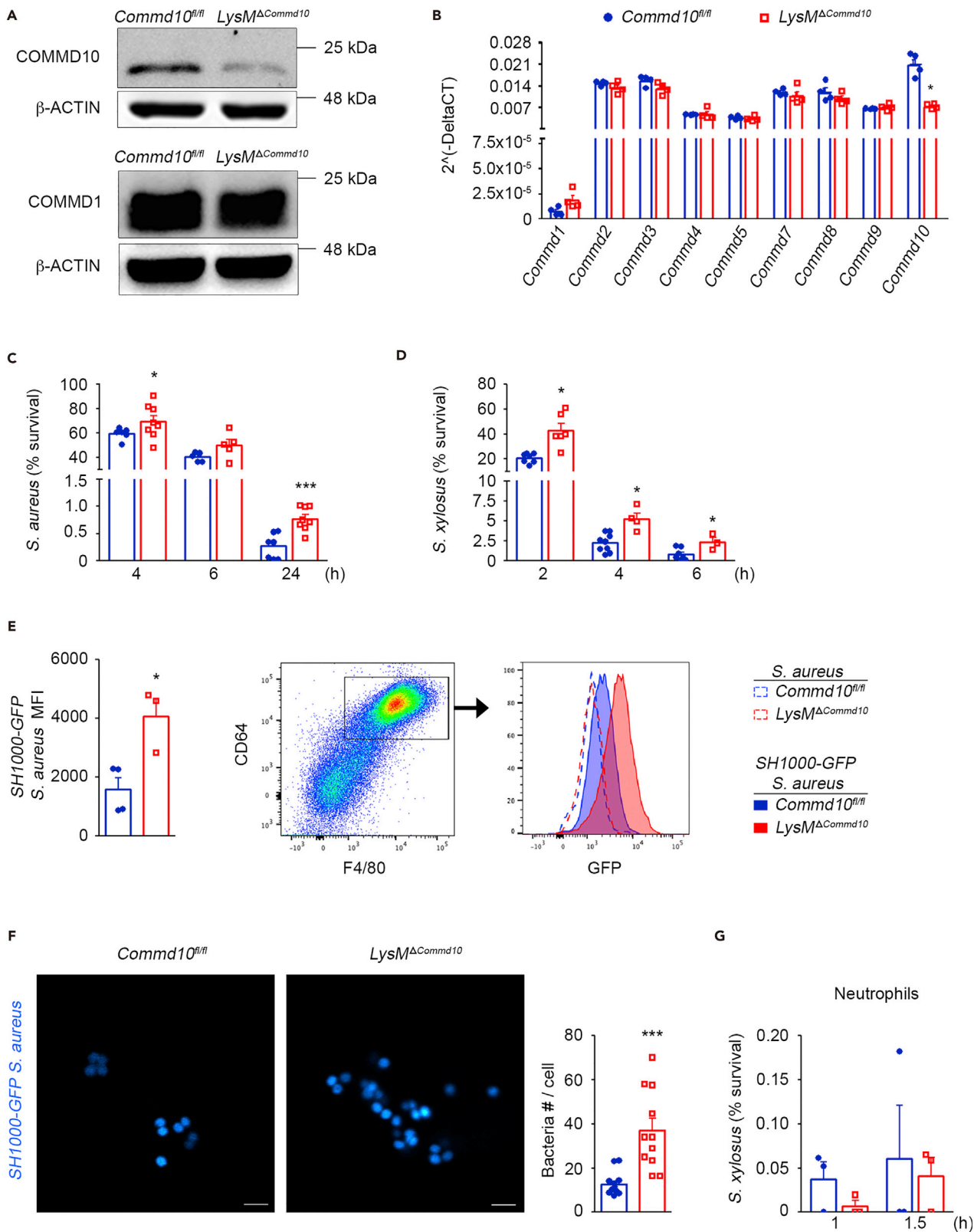


### Figure 2. Impaired Clearance of *S. aureus* in COMMD10-Deficient Macrophages

BMDM from *Commd10<sup>fl/fl</sup>* (blue, closed circles) or *LysM<sup>dCommd10</sup>* (red, open squares) mice were infected with *S. aureus* or *S. xyloso* at MOI = 5.

(A) Immunoblots showing the expression of COMMD10 and COMMD1 proteins.  $\beta$ -Actin was used as a control (n = 2).

(B) qRT-PCR gene expression of various COMMD members (n = 3).

(C and D) Survival over time in BMDM of (C) *S. aureus* (n  $\geq$  5) and (D) *S. xyloso* (n  $\geq$  3), as assessed by gentamycin protection assay.

(E) Left panel: average mean fluorescent intensity (MFI, calculated by subtracting background MFI of BMDM infected with wild-type *S. aureus* from MFI of BMDM infected with *SH1000-GFP S. aureus*) at 2 h post infection (n  $\geq$  3). Right panel: flow cytometry image showing gating strategy of BMDM (defined as CD64<sup>+</sup>F4/80<sup>+</sup>) and a histogram showing overlay of GFP fluorescence in *Commd10<sup>fl/fl</sup>* (blue) or *LysM<sup>dCommd10</sup>* (red) BMDM at 2 h following infection with non-labeled *S. aureus* (dashed lines) or *SH1000-GFP S. aureus* (filled lines).

(F) Confocal microscopic images showing internalized GFP-labeled *S. aureus* (cyan) at 4 h post infection. Magnification,  $\times$ 40; scale bar, 2  $\mu$ M (n  $\geq$  10 imaged cells per group [n  $\geq$  3]). Right: graph showing bacterial quantification.

(G) Survival of *S. xyloso* over time in BM-derived neutrophils as assessed by gentamycin protection assay (n = 4).

Data in (B), (E), and (G) were analyzed by non-parametric Mann-Whitney test, and data in (C–D) and (F) were analyzed by unpaired, two-tailed t test comparing each time between *Commd10<sup>fl/fl</sup>* and *LysM<sup>dCommd10</sup>*. Results are presented as mean  $\pm$  SEM with significance: \*p < 0.05 and \*\*\*p < 0.001.

GFP-tagged *S. aureus* (Figure 3B) or engulfed fluorescently labeled *S. aureus*-coated bioparticles (Figure 3C). Similar internalization of *S. aureus*-coated bioparticles was also corroborated by confocal microscopy analysis (Figure 3D). Hence, these results suggest that COMMD10 does not play a critical role in mediating *S. aureus* internalization.

### Lysosomal Biogenesis Is Impaired in *S. aureus*-Infected COMMD10-Deficient Macrophages

Phagolysosome-mediated cellular clearance processes require the concerted action of hydrolases, the acidification machinery, and membrane proteins. The expression and activity of these components must be coordinated to allow optimal phagolysosomal function during infection and relies on transcriptional regulation of a lysosomal gene network (Settembre et al., 2013). We hypothesized that the attenuated *S. aureus* clearance in COMMD10-deficient macrophages may be due to impaired lysosomal biogenesis. Indeed, gene expression profiling of BMDM at distinct time points following *S. aureus* infection uncovered altered expression of structural and functional lysosomal genes, whereas no significant differences were observed at baseline (Figure 4A). Accordingly, late phagosomes and lysosomes are normally enriched in lysosomal-associated membrane proteins (LAMP) 1 and 2 as well as lysosome membrane protein 2 (LIMP2, *Scarb2*) (Flannagan et al., 2009). COMMD10 deficiency resulted in significantly reduced expression of both *Lamp1* and *Lamp2* at 2 h and of *Scarb2* at 4 h following infection (Figure 4A). With respect to functional lysosomal genes, expression of cathepsins B and D (*Ctsb* and *Ctsd*, respectively) was reduced in COMMD10-deficient BMDM at 2 and 4 h following *S. aureus* infection, whereas cathepsin K (*Ctsk*) expression remained unchanged (Figure 4A). Gene expression of lysosomal acid lipase A (*Lipa*) was markedly lower at 2, 4, and 6 h following infection (Figure 4A). Acid phosphatase 5 is a lysosomal di-iron protein important for the clearance of *S. aureus* infection by mononuclear phagocytes (Bune et al., 2001). Its gene expression was also profoundly reduced at 6 h following infection (Figure 4A). Importantly, BMDM also exhibited reduced gene expression of the inflammatory cytokines interleukin (IL)-1 $\beta$  (*Il1b*) and IL-6 (Figure 4A). In agreement with this, supernatants from *S. aureus*- and *S. xyloso*-infected BMDM contained lower levels of secreted IL-1 $\beta$  (Figures 4B and 4C).

The transcription factor EB (TFEB) is a master inducer of lysosomal biogenesis (Sardiello et al., 2009). Phagocytosis enhances lysosomal and bactericidal activity in macrophages by activating TFEB translocation from the cytosol to the nucleus to facilitate a boost of the lysosome gene network (Gray et al., 2016). In macrophages infected with *S. aureus*, TFEB also induces the transcription of pro-inflammatory cytokines (Visvikis et al., 2014). In accordance with the reduced expression of lysosomal genes and of the cytokines IL-1 $\beta$  and IL-6 (Figure 4A), TFEB translocation to the nucleus was impaired in COMMD10-deficient versus COMMD10-proficient macrophages (Figure 4D). Moreover, activation of the master growth regulator mammalian target of rapamycin (mTOR) complex 1 (mTORC1), which inhibits TFEB nuclear translocation (Settembre et al., 2012), was higher in COMMD10-deficient macrophages at 2, 4 and 6 h following *S. aureus* infection as manifested by increased phosphorylation (Figure 4E). In aggregate, these results indicate a role for COMMD10 in promoting TFEB activation and associated lysosomal biogenesis.

### Retarded Lysosomal Maturation in *S. aureus*-Infected COMMD10-Deficient Macrophages

The nascent phagosome acquires the microbicidal and degradative capacities required for pathogen elimination by a process called *phagosome maturation* (Fairn and Grinstein, 2012; Flannagan et al., 2009). The attenuated clearance of *S. aureus* in COMMD10-deficient KCs (Figure 1) and macrophages (Figure 2)

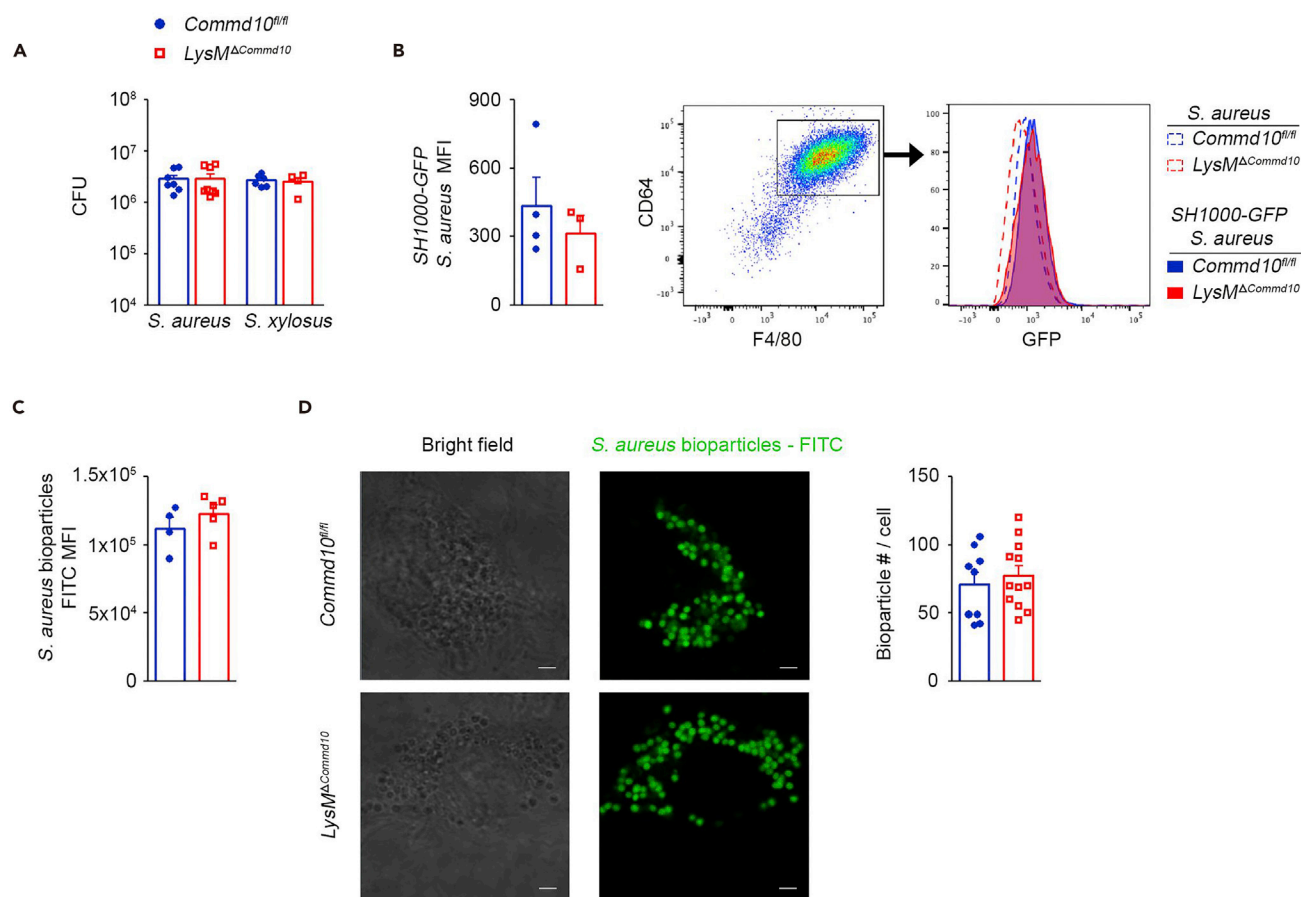


### Figure 3. COMMD10 Deficiency in Macrophages Does not Affect *S. aureus* Internalization

BMDM from *Commd10<sup>fl/fl</sup>* (blue, closed circles) or *LysM<sup>ΔCommd10</sup>* (red, open squares) mice were infected with *S. aureus* or *S. xylopus* at MOI = 5 for 30 min. (A) Baseline internalization and survival at 30 min post infection of *S. aureus* (n = 8) and *S. xylopus* (n = 6), as assessed by gentamycin protection assay.

(B) Average mean fluorescent intensity (MFI, calculated by subtracting background MFI of BMDM infected with WT *S. aureus* from MFI of BMDM infected with SH1000-GFP *S. aureus*) at 30 min post infection (n ≥ 3). Right panel: flow cytometry image showing gating strategy for BMDM (defined as CD64<sup>+</sup>F4/80<sup>+</sup>) and a histogram showing overlay of GFP fluorescence in *Commd10<sup>fl/fl</sup>* (blue) or *LysM<sup>ΔCommd10</sup>* (red) BMDM at 30 min following infection with non-labeled *S. aureus* (dashed lines) or SH1000-GFP *S. aureus* (filled lines).

(C) Average MFI of fluorescein-coated *S. aureus* bioparticles after 3-h incubation (n = 5).

(D) Confocal microscopy images showing internalized fluorescein-coated *S. aureus* bioparticles (green) at 3 h post incubation. Magnification, ×40; scale bar, 2 μm (n ≥ 10 cells per group). Right: graph showing bacterial quantification.

Data were analyzed by non-parametric Mann-Whitney test, comparing each time between *Commd10<sup>fl/fl</sup>* and *LysM<sup>ΔCommd10</sup>*, and are presented as mean ± SEM.

together with the impaired lysosomal biogenesis (Figure 4) may indicate defective phagolysosomal maturation. The Rab-family GTPases are known to mediate the progression between the early, late, and lysosome fusion stages. Specifically, Rab5 is a characteristic marker of the early phagosome that drives the transition to the late phagosome stage, which is defined by the presence of Rab7 (Harrison et al., 2003; Vieira et al., 2003). The expression of RAB5 was profoundly higher in COMMD10-deficient macrophages at 2 and 4 h following infection, whereas RAB7 protein was significantly reduced (Figure 5A). In addition, there was a decline in the protein expression of Rabaptin-5 (Figure 5A), which is an essential and rate-limiting component for early endosome fusion (Horiuchi et al., 1997; Lippe et al., 2001). The expression of LAMP1, a characteristic marker of late phagosomes and phagolysosomes (Flannagan et al., 2009), was also significantly reduced at 4 h following infection (Figure 5A). Of note, there was no clear difference in the expression of LAMP1, RAB7, and RAB5 at the basal level (Figure S2), suggesting that COMMD10 is not involved with their homeostatic regulation. Confocal microscopic imaging at 1 h following *S. aureus* infection of macrophages further revealed that the recruitment of LAMP1 to bacteria containing late phagosomes or phagolysosomes depends on COMMD10. Accordingly, whereas in COMMD10-proficient macrophages LAMP1

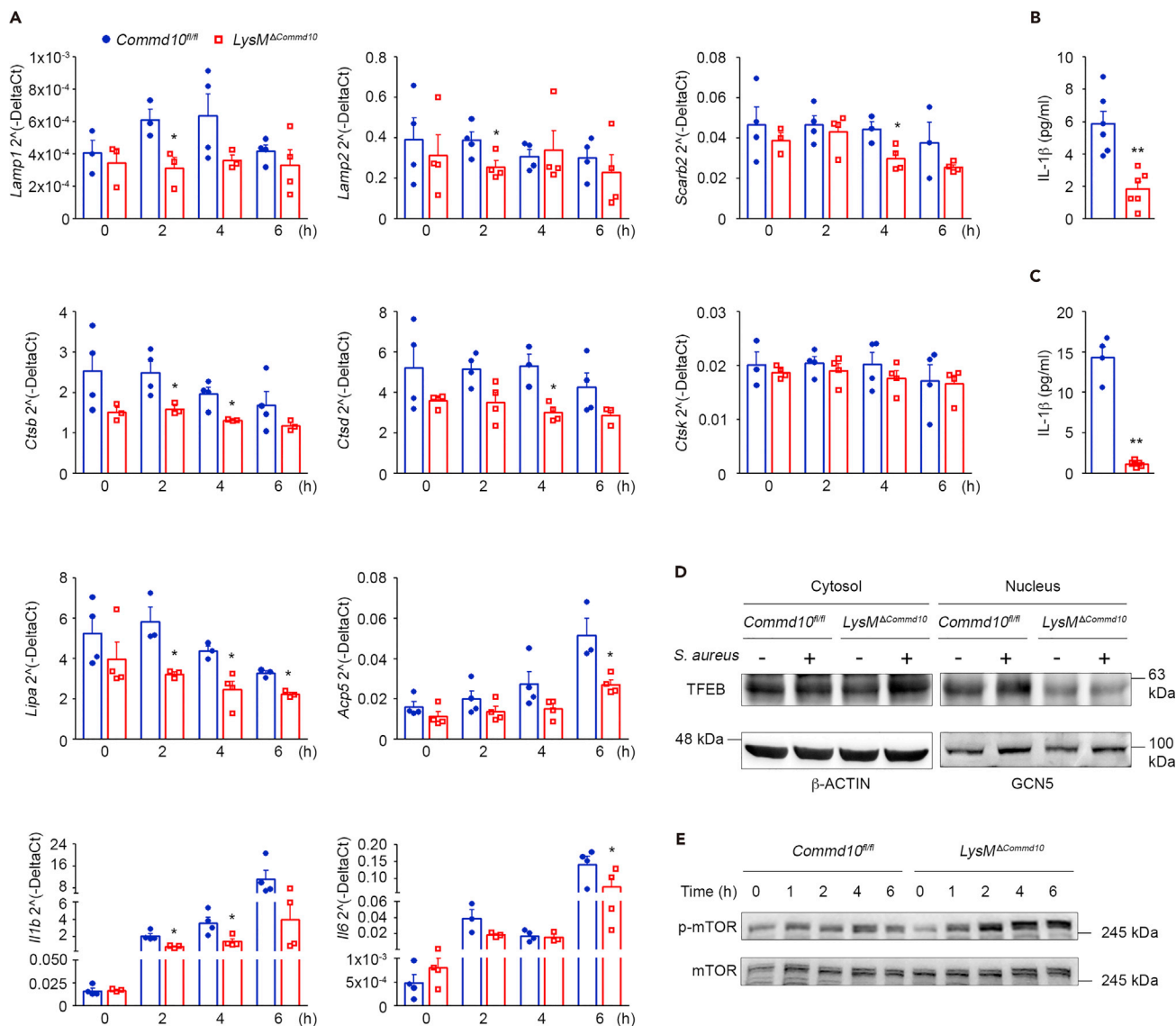


**Figure 4. *S. aureus*-infected COMMD10-deficient macrophages exhibit impaired TFEB-associated lysosomal biogenesis**

BMDM from *Commd10<sup>fl/fl</sup>* (blue, closed circles) or *LysM<sup>ΔCommd10</sup>* (red, open squares) mice were infected with *S. aureus* at MOI = 5 (A and B) or 10 (D and E) or with *S. xyloso* at MOI = 5 (C). (A) qRT-PCR gene expression over time of lysosomal and inflammatory genes (n = 4). (B–C) Cell-free supernatants were subjected to ELISA analysis of IL-1β following (B) *S. aureus* and (C) *S. xyloso* infection (n = 6 for B, n ≥ 4 for C). (D) Immunoblots showing TFEB expression in cytosolic and nuclear fraction lysates of non-infected or *S. aureus*-infected BMDM. β-Actin and GCN5 antibodies, respectively, were used as controls (n ≥ 5). (E) Immunoblots demonstrating the expression of phospho-mTOR and mTOR in BMDM lysates over a time course post *S. aureus* infection (n ≥ 3). Data in (A) and (C) were analyzed by non-parametric Mann-Whitney test and data in (B) were analyzed by unpaired, two-tailed t test, comparing each time between *Commd10<sup>fl/fl</sup>* and *LysM<sup>ΔCommd10</sup>* BMDM. Results are presented as mean ± SEM with significance: \*p < 0.05, \*\*p < 0.01.

enveloped *S. aureus*-containing phagolysosomes, it was mostly mislocalized to the cell surface membrane in the COMMD10-deficient macrophages (Figure 5B). Similarly to LAMP1, staining for COMMD10 localized its expression to the *S. aureus*-containing phagolysosomal membrane (Figure 5C). Altogether, these results suggest that COMMD10-deficient phagosomes are detained at an early maturation phase.

### COMMD10-Deficient Macrophages Exhibit Impaired Phagolysosomal Acidification in Response to *S. aureus* Infection

The attenuated phagolysosomal maturation in *S. aureus*-infected COMMD10-deficient macrophages (Figure 5) may lead to impaired acquisition of bactericidal features. Concomitant with phagosome maturation

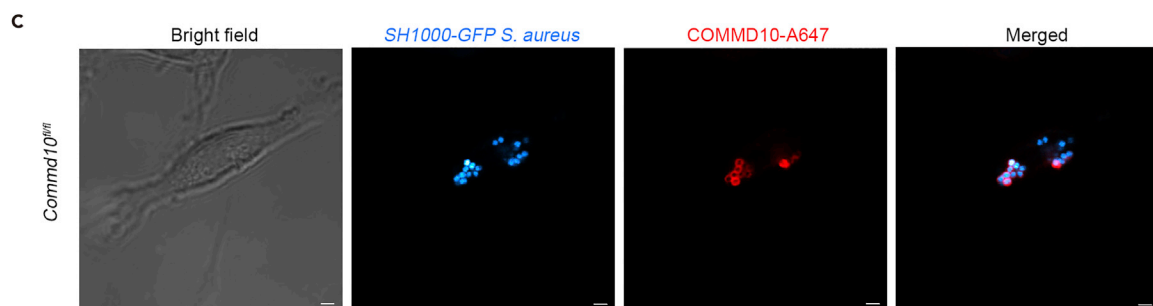
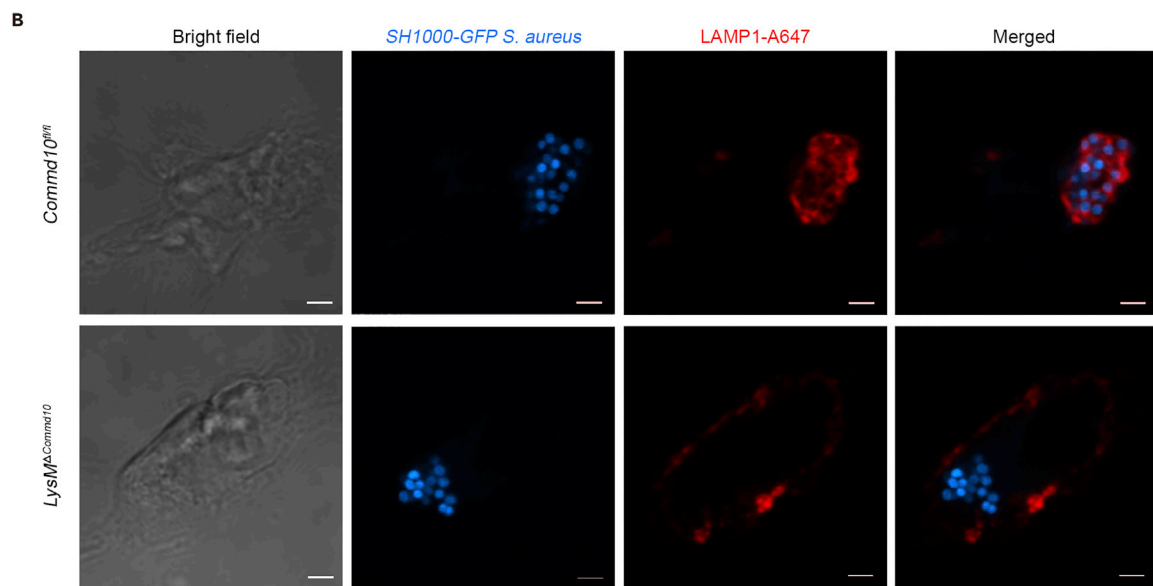
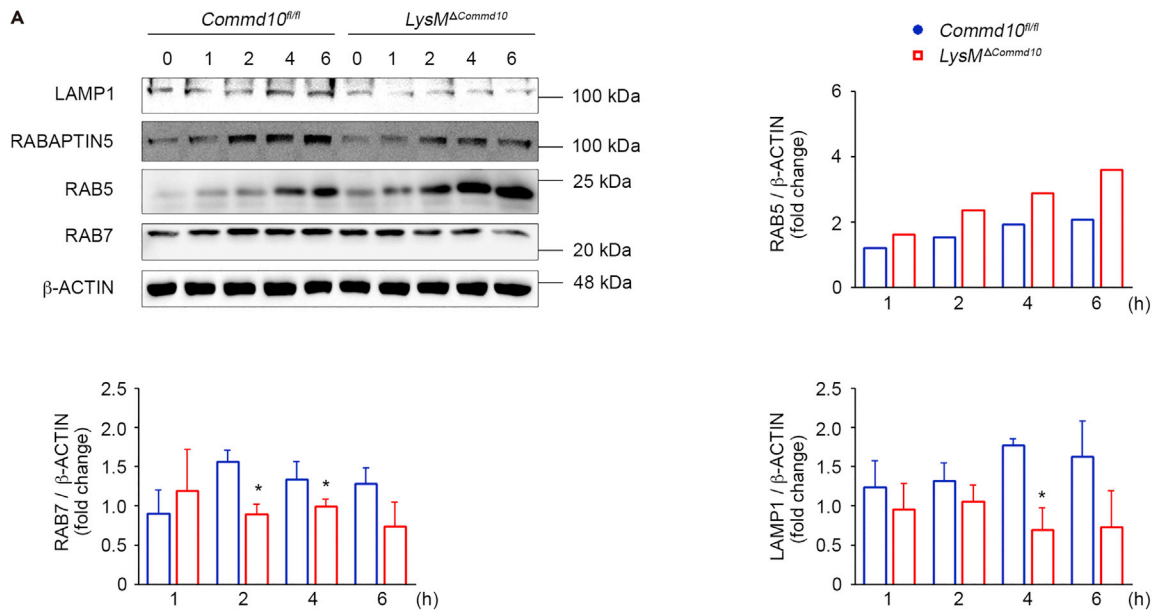


### Figure 5. Impaired Lysosomal Maturation in *S. aureus*-Infected COMMD10-Deficient Macrophages

BMDM from *Commd10<sup>fl/fl</sup>* (blue, closed circles) or *LysM<sup>d</sup>Commd10* (red, open squares) mice were infected with (A) untagged or (B) *SH1000-GFP S. aureus* at MOI = 5.

(A) Immunoblots showing the expression of indicated phagolysosome proteins.  $\beta$ -Actin served as control. Densitometry is presented on the right and bottom panels ( $n \geq 3$ ).

(B) Confocal microscopic images showing co-localization of *SH1000-GFP S. aureus* (cyan) and LAMP-1 (red) at 1 h post infection. Magnification,  $\times 100$ ; scale bar, 2  $\mu$ M.

(C) Confocal microscopy images showing COMMD10 staining (red) together with internalized *S. aureus* (cyan). Magnification,  $\times 40$ ; scale bar, 2  $\mu$ M ( $n \geq 10$  cells per group).

Data were analyzed by unpaired, two-tailed t test, comparing each time between *Commd10<sup>fl/fl</sup>* and *LysM<sup>d</sup>Commd10* BMDM. Results are presented as mean  $\pm$  SEM with significance: \* $p < 0.05$ .

is the progressive acidification of the phagosome lumen, which aids the killing and digestion of intracellular *S. aureus* in macrophages (Jubrail et al., 2016). Confocal microscopic analysis of macrophages at 1 h following infection with *S. aureus* conjugated with the pH-sensitive pHrodo indicator revealed a significantly reduced fraction of pHrodo<sup>bright</sup> phagolysosomes out of total phagolysosomes in the COMMD10-deficient versus COMMD10-proficient macrophages (Figure 6A). Comparable results were achieved with GFP-tagged *S. aureus* (data not shown). The fraction of pHrodo<sup>bright</sup> *S. aureus*-containing phagolysosomes was similar to that of *Commd10<sup>fl/fl</sup>* macrophages pretreated with the V-ATPase inhibitor bafilomycin A (Figure 6A). This was confirmed by the reduced pHrodo signal in the COMMD10-deficient macrophages at 2 and 4 h following infection (Figure 6B). Labeling with LysoTracker further consolidated the reduction in acidic organelles in the COMMD10-deficient macrophages at 1 h following *S. aureus* infection (Figure 6C). Activation of the nicotinamide adenine dinucleotide phosphate (NADPH) oxidase (NOX) and the resulting reactive oxygen species (ROS) production neutralizes the acidification of the phagolysosome (Hampton et al., 1998; Savina et al., 2006; Segal et al., 1981). Therefore the impaired phagosome acidification in *S. aureus*-infected COMMD10-deficient macrophages may be the result of increased NOX activity. Indeed, assessment of ROS production revealed increased fraction of ROS<sup>+</sup> macrophages at 2 and 4 h following *S. aureus* infection (Figure 6D). As NOX-2 complex is a key driver of ROS production (Panday et al., 2015), we next assessed the expression of the cytochrome *b* (*Cybb*) subunit following *S. aureus* infection. Despite the increased production of ROS in COMMD10-deficient BMDM, their expression of *Cybb* was similar to that of *Commd10<sup>fl/fl</sup>* macrophages in steady state and at distinct time points following *S. aureus* infection (Figure 6E). Acidification is a prerequisite for the function of most lysosomal hydrolases, such as cathepsin D (Sturgill-Koszycki et al., 1996). In the absence of COMMD10, *S. aureus*-infected macrophages displayed reduced levels of activated cathepsin D (Figure 6F) and attenuated cathepsin D activity (Figure 6G). Altogether, these results uncover that COMMD10 deficiency in macrophages impairs phagolysosomal acidification and function in response to *S. aureus* infection.

### COMMD10-Deficient Macrophages Display Reduced Stability of the CCC Complex

Different COMMD proteins were found, in human cells, to be part of the CCC protein complex, which facilitates intracellular cargo-specific trafficking via interaction with the endolysosomal system (Li et al., 2015; Phillips-Krawczak et al., 2015; Starokadomskyy et al., 2013). In particular, CCC interacts with the WASH complex (Bartuzi et al., 2016; Phillips-Krawczak et al., 2015), which is involved with both bacterial phagocytosis (Buckley et al., 2016) and lysosomal recycling (King et al., 2013). Therefore the impaired phagolysosomal maturation and clearance of *S. aureus* in COMMD10-deficient macrophages may be related to defects in CCC complex stability. Indeed, analysis of COMMD10-deficient macrophages revealed reduced gene and protein expression of CCDC93 and CCDC22, components of the CCC complex, as well as of the CCC-associated protein C16ORF62, both at steady state and following *S. aureus* infection (Figures 7A and 7B). Therefore COMMD10-CCC complex interactions may be involved in the trafficking and fusion events required for *S. aureus* elimination in macrophages.

## DISCUSSION

We report here by using two different *S. aureus* subspecies that COMMD10 in macrophages is pivotal for timely handling of the Gram<sup>pos</sup> bacteria *S. aureus*. We show that COMMD10 is important for the barrier function of KCs against circulating *S. aureus*. Both COMMD10-deficient primary KCs and BMDM exhibited impaired clearance of *S. aureus* infection. The failure of KCs to eliminate *S. aureus* infection *in vivo* was translated into exacerbated hepatic damage and systemic disease. *S. aureus* internalization was unaltered by COMMD10 deficiency, whereas phagolysosomal biogenesis and maturation were significantly attenuated. In particular, there was reduced activation of the master lysosomal biogenesis transcription regulator

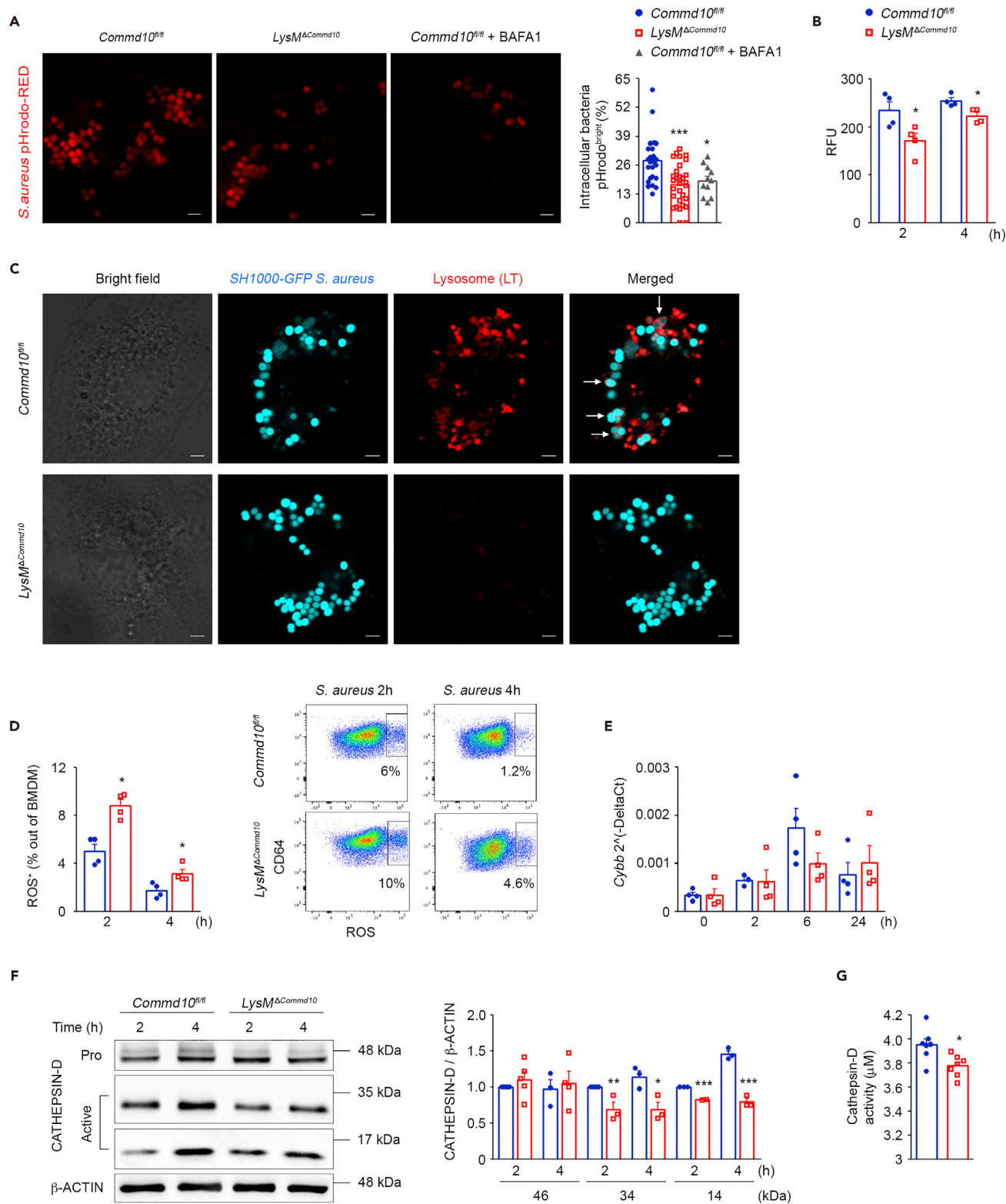


**Figure 6. COMMD10-Deficient Macrophages Exhibit Impaired Lysosomal Killing Machinery upon *S. aureus* Infection**

BMDM from Commd10<sup>fl/fl</sup> (blue, closed circles) or LysM<sup>ΔCommd10</sup> (red, open squares) mice were infected with pHrodo-labeled (red) (A and B) or GFP-labeled (cyan) (C) *S. aureus* at MOI = 20 or unlabeled (D–F) *S. aureus* at MOI = 5. (A) Confocal microscopic images showing intracellular bacteria at 1 h post infection,

**Figure 6. Continued**

pHrodo-positive bacteria are bright red. BafilomycinA (BAFA1) was used as positive control in *Commd10<sup>fl/fl</sup>* BMDM. Magnification,  $\times 63$ ; scale bar,  $2\ \mu\text{M}$  ( $n \geq 30$  cells per group). Right panel, pHrodo<sup>bright</sup> *S. aureus* per cell are presented as percentage of total intracellular bacteria per cell. Data are derived from two independent experiments. (B) Relative fluorescence unit (RFU) of pHrodo-labeled *S. aureus* at indicated time points post infection as assessed by fluorescent plate reader ( $n = 4$ ). (C) Confocal microscopic images showing co-localization (as marked by white arrows) of intracellular bacteria (cyan) with acidic compartments (stained with LysoTracker, red) at 1 h post infection. Magnification,  $\times 63$ ; scale bar,  $2\ \mu\text{M}$  ( $n \geq 30$  cells per group). (D) Fraction of ROS<sup>+</sup> BMDM at 2 and 4 h post infection, as assessed by flow cytometry using DCFH-DA ( $n = 4$ ). Right panel, representative flow cytometry images showing ROS fluorescence. (E) *Cybb* expression at baseline and following *S. aureus* infection as determined by qRT-PCR ( $n = 4$ ). (F) Left panel: immunoblots showing expression of pro- (46 kDa) and activated (34 and 14 kDa) cathepsin D over time.  $\beta$ -Actin was utilized as control ( $n = 5$  for 34 and 46 kDa,  $n = 3$  for 14 kDa). Densitometry is presented on the right. (G) Cathepsin D-degrading activity (HiLyte Fluor-488  $\mu\text{M}$ ) 2 h post infection as assessed by fluorescent plate reader ( $n = 7$ ). Data in (A) were analyzed by one-way ANOVA with Tukey post test, comparing between *Commd10<sup>fl/fl</sup>* and *LysM<sup>dCommd10</sup>* or *Commd10<sup>fl/fl</sup>* + BAFA1. Data in (B), (D), and (E) were analyzed by non-parametric Mann-Whitney test and data in (F–G) were analyzed by unpaired, two-tailed t test, comparing each time between *Commd10<sup>fl/fl</sup>* and *LysM<sup>dCommd10</sup>* BMDM. Results are presented as mean  $\pm$  SEM with significance: \* $p < 0.05$ , \*\* $p < 0.01$ , \*\*\* $p < 0.001$ .

TFEB concomitantly with reduced expression of its associated genes encoding for lysosomal structural and functional proteins. Moreover, there was a delay in the acquisition of mature phagolysosomal markers. COMMD10-deficient macrophages also exhibited reduced phagolysosomal acidification coupled with augmented production of lysosome-neutralizing ROS. Finally, we show reduced representation of the CCC complex genes and proteins in macrophages deficient in COMMD10.

COMMD proteins have been linked to the endolysosomal system. COMMD1, the most studied prototype of this family, functions as part of the CCC complex. Similarly, studies in HEK cells have shown that COMMD10 binds the CCDC22 component of the CCC complex (Starokadomskyy et al., 2013). This complex localizes to endosomes and interacts with the WASH complex (Bartuzi et al., 2016; Phillips-Krawczak et al., 2015). The latter regulates the actin cytoskeleton by modulating Arp2/3-governed actin polymerization in immune cells and thus is important to multiple aspects of immune cell function (Thrasher and Burns, 2010). Specifically, it is intimately linked to bacterial phagocytosis by mononuclear phagocytes, for instance, via its modulation of phagocytic cup formation (Lorenzi et al., 2000; Tsuboi and Meerloo, 2007). Yet, we did not observe an effect for COMMD10 deficiency on *S. aureus* internalization. WASH is also required for efficient phagolysosomal maturation by governing delivery of lysosomal hydrolases. Moreover, in cells lacking WASH, cathepsin D becomes trapped in a late endosomal compartment, unable to be recycled to nascent phagosomes and autophagosomes (King et al., 2013). We see reduced gene and protein expression of CCC complex members in the COMMD10-deficient BMDM at steady state and following *S. aureus* infection. These cells also display reduced levels of activated cathepsin D. These findings suggest that COMMD10-CCC-WASH interactions may be required for adequate maturation and recycling of *S. aureus* containing phagosomes.

TFEB is a master transcription factor that induces transcription of lysosomal biogenesis genes that share a common CLEAR motif such as LAMP1 and 2 and cathepsins (Sardiello et al., 2009). The inhibition of mTOR is required for cytosolic dephosphorylation of TFEB, facilitating its nuclear translocation (Settembre et al., 2012). TFEB activation occurs in response to nutritional shortage leading to autophagy (Settembre et al., 2011), and also in macrophages exposed to LPS or bacterial infection (Gray et al., 2016; Visvikis et al., 2014; Vural et al., 2016). In particular, during *S. aureus* infection, macrophages with constitutively high TFEB activity have improved survival (Vural et al., 2016). Consistent with the impaired ability of COMMD10-deficient macrophages to clear *S. aureus* infection, we found that they exhibit repressed TFEB nuclear translocation and suppressed transcription of TFEB-mediated lysosomal genes. Furthermore, TFEB-mediated transcription is not limited to lysosomal biogenesis but is directed at over 400 target gene sites governing, among other processes, endocytosis, autophagy, essential protein degradation, and immune responses (Palmieri et al., 2011). Regarding the latter, in macrophages exposed to *S. aureus*, TFEB drives the production of inflammatory cytokines essential for adequate host defense such as IL-6 and IL-1 $\beta$  as well as antimicrobial peptides (Visvikis et al., 2014). In line with their repressed TFEB nuclear translocation, COMMD10-deficient macrophages infected with *S. aureus* had less expression and secretion of inflammatory cytokines, potentially compromising their ability to kill bacteria.

Nascent phagosomes must undergo maturation to acquire microbicidal properties required for elimination of engulfed pathogens (Fair and Grinstein, 2012; Flannagan et al., 2009). Our results highlight a pivotal role for COMMD10 in timely and proper phagolysosomal maturation following *S. aureus* infection. Accordingly, COMMD10-deficient macrophages displayed impaired exchange of RAB5 to RAB7 and

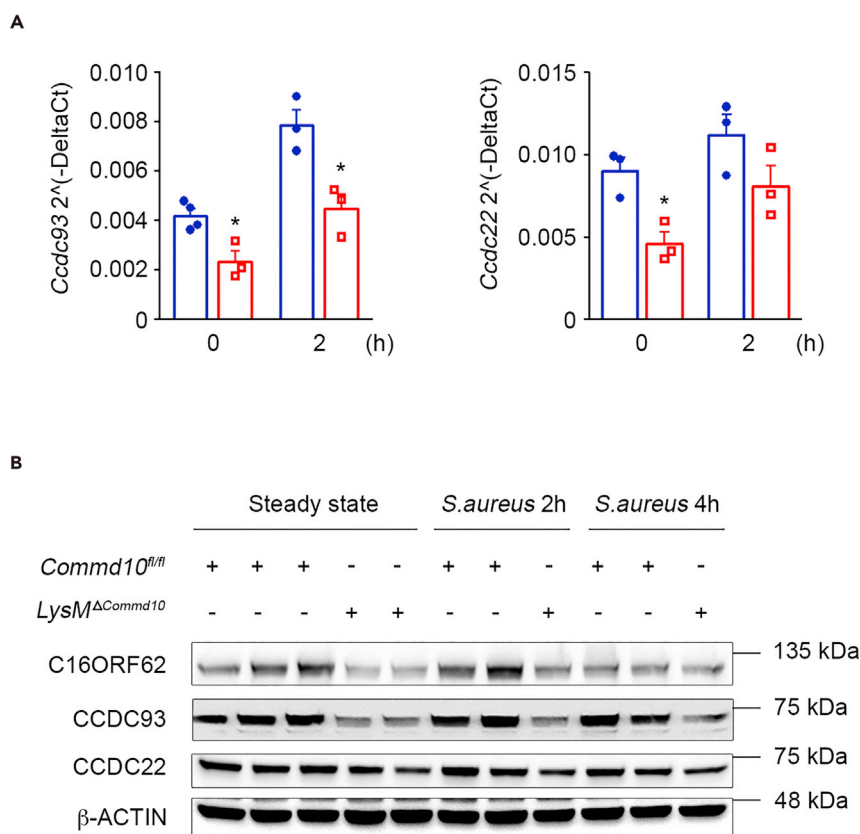


### Figure 7. COMMD10-Deficient Macrophages Display Reduced Stability of the CCC Complex

BMDM from *Commd10*<sup>fl/fl</sup> (blue, closed circles) or *LysM*<sup>Δ*Commd10*</sup> (red, open squares) mice were infected with *S. aureus* at MOI = 5.

(A) *Ccdc93* and *Ccdc22* expression at baseline and following *S. aureus* infection as determined by qRT-PCR (n = 4).

(B) Immunoblots demonstrating expression of CCDC93, CCDC22, and C16ORF62 in BMDM lysates at baseline and post *S. aureus* infection. β-Actin was utilized as control (n = 2 independent experiments).

Data were analyzed by non-parametric Mann-Whitney test. Results are presented as mean ± SEM with significance:

\*p < 0.05.

reduced expression and mislocation of LAMP1 to the cell membrane rather than the phagosomal membrane. Peripheral lysosomes have reduced RAB7 density and are associated with reduced acidification and impaired proteolytic activity when compared with juxtannuclear ones (Johnson et al., 2016). Given the peripheral localization of LAMP1 and reduced RAB7 levels in the COMMD10-deficient BMDM, these results may indicate that their phagolysosomes are less bactericidal.

A hallmark of phagolysosome formation is the marked acidification of the phagosome lumen due to the activity of the vacuolar ATPase (V-ATPase) proton pump (Lukacs et al., 1990). Despite the antimicrobial activity of the macrophage phagolysosome, some *S. aureus* survive within mature phagolysosomes by virtue of various virulence factors and regulators, where their replication commences before cell death (Flannagan et al., 2016, 2018; Pollitt et al., 2018; Surewaard et al., 2016). In fact, it has been recently shown for the *S. aureus* USA300 strain that its exposure to acidic pH evokes signaling pathways that endow the bacteria with increased resistance to antimicrobial effectors, such as antimicrobial peptides encountered inside macrophage phagolysosomes (Flannagan et al., 2018). Therefore, although the compromised phagolysosomal acidification in COMMD10-deficient macrophages can assist the *S. aureus* in evading killing, it may in parallel hamper its induction of pH-dependent adaptive survival responses and subsequent replication in these cells. However, replication of *S. aureus* in macrophages occurs after a significant delay (~10–12 h) (Flannagan et al., 2016; Surewaard et al., 2016). In contrast, our *in vivo* data reveal significant reductions in the level of KCs already after 3 h, suggesting that they succumb to the bacteria before their replication

commences. Moreover, it remains unclear whether pH-dependent survival mechanisms described for the USA300 *S. aureus* strain are also a feature of the Rosenbach and SH1000 strains used here. Further studies are required to follow the effect of COMMD10 deficiency on the dynamics of *S. aureus* survival and replication within KCs.

One explanation for the reduced acidification of phagolysosomal compartments in COMMD10-deficient macrophages is their augmented production of ROS, which neutralize the acidification of phagolysosomes (Hampton et al., 1998; Savina et al., 2006; Segal et al., 1981). However, ROS production is an important mechanism in combating *S. aureus*. Indeed, patients with chronic granulomatous disease having defective ROS production are prone to recurrent life-threatening staphylococcal infections and persistent inflammation (Buvelot et al., 2017). Although increased ROS production would normally be expected to result in more effective bacterial handling, *S. aureus* may be an exception, as it is known to express anti-oxidant enzymes, such as catalase and superoxide dismutase, that confer resistance to ROS in macrophages (Das and Bishayi, 2009, 2010). It is still unclear how COMMD10 regulates ROS production. Expression of *Cybb* was unchanged in COMMD10-deficient macrophages. Although expression of other NOX2 complex subunits should be examined, these results suggest the possibility of transcription-independent mechanisms. Alternatively, given the involvement of COMMD proteins in intracellular protein trafficking events, COMMD10 may be important for controlling the assembly and stability of NOX2 multi-domain complex and its translocation from the cytosol to the membrane.

Although our results underscore an important role for COMMD10 in promoting TFEB-governed lysosomal biogenesis at 2–4 h following *S. aureus* infection, they also indicate profound alterations in phagolysosomal maturation events occurring at earlier time points, as manifested by impaired recruitment of LAMP1 to phagolysosomes, exchange of RAB5 to RAB7, phagolysosomal acidification, and cathepsin D activity. These alterations seem too rapid to be transcription mediated and may be related to the effect of COMMD10 deficiency on protein trafficking events. Indeed, COMMD10 has been associated with phagosomes in macrophages (Dill et al., 2015), and we show here the recruitment of COMMD10 protein to *S. aureus* containing phagolysosomes already at 1 h following infection. Moreover, macrophages with COMMD10-deficiency exhibit reduced expression of CCC complex genes and proteins. This complex modulates endolysosome architecture and is required for the correct trafficking of diverse transmembrane proteins that traverse this compartment. Hence impaired COMMD10-CCC interactions may be important for the trafficking events driving phagolysosomal maturation, function, and recycling. Given the persistent survival of *S. aureus* in macrophages (Flannagan et al., 2016, 2018; Jubrail et al., 2016; Pollitt et al., 2018; Surewaard et al., 2016), the process of phagolysosomal biogenesis, maturation, and recycling is dynamic and continuous, therefore necessitating both ongoing transcriptional and protein trafficking regulation by COMMD10.

To target COMMD10 deficiency to KCs *in vivo* we utilized *Cx3cr1<sup>cre</sup>* mice (Yona et al., 2013). In these mice, cre-driven recombination (and the ensuing COMMD10 deficiency) is largely restricted in the liver to KCs (Yona et al., 2013), as well as to CX<sub>3</sub>CR1<sup>+</sup> LCMs (Sierra et al., 2017) and a subset of dendritic cells (David et al., 2016). Here we show that LCMs also express COMMD10, and hence their altered activity in the setting of COMMD10 deficiency may contribute to the overall phenotype observed in the *Cx3cr1<sup>ΔCommd10</sup>* livers. In this regard, it has been shown that KCs are mainly responsible for the clearance of bacteria originating from the circulation, whereas LCMs are in charge of handling pathogens traversing the peritoneum (Sierra et al., 2017). Indeed, circulating *S. aureus* are rapidly killed by KCs (Pollitt et al., 2018; Surewaard et al., 2016). Therefore, although it remains to be examined, we expect that COMMD10 deficiency in LCMs does not directly impair the clearance of blood-borne *S. aureus*. LCMs express various chemokines that may be involved in the sequential recruitment of immune cells such as neutrophils and Ly6C<sup>hi</sup> monocytes (Sierra et al., 2017). Our data reveal increased infiltration of Ly6C<sup>hi</sup> monocytes to *S. aureus*-infected *Cx3cr1<sup>ΔCommd10</sup>* livers at 24 h, but the respective contributions of KCs and LCMs to their recruitment remain to be determined. Moreover, it is also not clear whether COMMD10 deficiency in LCMs contributes to the overall increase in hepatocyte necrosis observed at the subcapsular zone of *Cx3cr1<sup>ΔCommd10</sup>* livers. We have previously shown that COMMD10 is important for the negative regulation of inflammasome activity in liver-infiltrating Ly6C<sup>hi</sup> monocytes during endotoxic shock in *Lyz2<sup>cre</sup>Commd10<sup>fl/fl</sup>* mice, but not *Cx3cr1<sup>ΔCommd10</sup>* mice (Mouhadeb et al., 2018). This is probably related to the greater activity of cre-recombinase in the ephemeral circulating Ly6C<sup>hi</sup> monocytes in the *Lyz2<sup>cre</sup>* versus *Cx3cr1<sup>cre</sup>* mice (Abram et al., 2014). Therefore, we believe that COMMD10 deficiency in Ly6C<sup>hi</sup> monocytes does not directly contribute to the overall impaired clearance of *S. aureus* infection in the *Cx3cr1<sup>ΔCommd10</sup>* livers, but may be involved to

some extent with the overall augmented hepatic damage observed after 24 h. Macrophages in the liver mediate the initial infecting *S. aureus* population bottleneck, whereas neutrophils enable the subsequent spread of bacteria to other organs (Pollitt et al., 2018). We have previously shown that circulating neutrophils hardly express COMMD10 (Mouhaddeb et al., 2018) and are *a priori* not a target for cre-recombination in the *Cx3cr1<sup>cre</sup>* mice (Abram et al., 2014). Moreover, neutrophil recruitment to the *S. aureus*-infected liver was not affected in the *Cx3cr1<sup>ΔCommd10</sup>* mice, and *LysM<sup>ΔCommd10</sup>* primary neutrophils exhibited unaltered handling of *S. xyloso*. Therefore these results rule out a contribution of neutrophils to the impaired clearance of *S. aureus* and collateral damage in the *Cx3cr1<sup>ΔCommd10</sup>* livers.

Altogether, we report a pivotal role for COMMD10 in macrophages in mediating lysosomal biogenesis and maturation in response to *S. aureus* infection and in upholding KC barrier function against *S. aureus* bacteremia.

### Limitations of the Study

To target COMMD10 deficiency to KCs *in vivo* we utilized *Cx3cr1<sup>cre</sup>* mice (Yona et al., 2013). Besides KCs, cre-driven recombination (and the ensuing COMMD10 deficiency) also targets liver CX<sub>3</sub>CR1<sup>+</sup> LCMs (Sierro et al., 2017) and a subset of dendritic cells (David et al., 2016). This caveat has been extensively elaborated on in the discussion. Although we cannot exclude a contribution of other liver CX<sub>3</sub>CR1<sup>+</sup> cells to *in vivo* phenotypes observed in this study, we have complemented our *in vivo* observations by comprehensive *in vitro* studies directly characterizing the effects of COMMD10 deficiency on *S. aureus* handling mechanisms in primary cell cultures of KCs and BMDMs.

### METHODS

All methods can be found in the accompanying Transparent Methods supplemental file.

### SUPPLEMENTAL INFORMATION

Supplemental Information can be found online at <https://doi.org/10.1016/j.isci.2019.03.024>.

### ACKNOWLEDGMENTS

The authors acknowledge support from the Israel Science Foundation (grant # 1777/13) and the Israel Ministry of Health (grant # 10052). This research was also supported by a Grant from the GIF, the German-Israeli Foundation for Scientific Research and Development (grant # 2094/09). Work in the Varol laboratory has been supported by the Azrieli Foundation Canada-Israel.

### AUTHOR CONTRIBUTIONS

S.B.S., O.M., C.V., and N.G. conceived the study, designed experiments, and wrote the manuscript. S.B.S., O.M., and K.C. performed the experiments and analyzed the data. N.G and C.V are co-corresponding authors. Both equally supervised the work and are responsible for all data presented and analyzed.

### DECLARATION OF INTERESTS

The authors declare no competing interests.

Received: October 24, 2018

Revised: February 28, 2019

Accepted: March 21, 2019

Published: April 26, 2019

### REFERENCES

Abram, C.L., Roberge, G.L., Hu, Y., and Lowell, C.A. (2014). Comparative analysis of the efficiency and specificity of myeloid-Cre deleting strains using ROSA-EYFP reporter mice. *J. Immunol. Methods* 408, 89–100.

Bartuzi, P., Billadeau, D.D., Favier, R., Rong, S., Dekker, D., Fedoseienko, A., Fieten, H., Wijers, M., Levels, J.H., Huijckman, N., et al. (2016). CCC-

and WASH-mediated endosomal sorting of LDLR is required for normal clearance of circulating LDL. *Nat. Commun.* 7, 10961.

Buckley, C.M., Gopaldass, N., Bosmani, C., Johnston, S.A., Soldati, T., Insall, R.H., and King, J.S. (2016). WASH drives early recycling from macropinosomes and phagosomes to maintain

surface phagocytic receptors. *Proc. Natl. Acad. Sci. U S A* 113, E5906–E5915.

Bune, A.J., Hayman, A.R., Evans, M.J., and Cox, T.M. (2001). Mice lacking tartrate-resistant acid phosphatase (Acp 5) have disordered macrophage inflammatory responses and reduced clearance of the pathogen,

- Staphylococcus aureus. *Immunology* 102, 103–113.
- Burstein, E., Hoberg, J.E., Wilkinson, A.S., Rumble, J.M., Csomos, R.A., Komarck, C.M., Maine, G.N., Wilkinson, J.C., Mayo, M.W., and Duckett, C.S. (2005). COMMD proteins, a novel family of structural and functional homologs of MURR1. *J. Biol. Chem.* 280, 22222–22232.
- Buvelot, H., Posfay-Barbe, K.M., Linder, P., Schrenzel, J., and Krause, K.H. (2017). Staphylococcus aureus, phagocyte NADPH oxidase and chronic granulomatous disease. *FEMS Microbiol. Rev.* 41, 139–157.
- Das, D., and Bishayi, B. (2009). Staphylococcal catalase protects intracellularly survived bacteria by destroying H<sub>2</sub>O<sub>2</sub> produced by the murine peritoneal macrophages. *Microb. Pathog.* 47, 57–67.
- Das, D., and Bishayi, B. (2010). Contribution of catalase and superoxide dismutase to the intracellular survival of clinical isolates of Staphylococcus aureus in murine macrophages. *Indian J. Microbiol.* 50, 375–384.
- David, B.A., Rezende, R.M., Antunes, M.M., Santos, M.M., Freitas Lopes, M.A., Diniz, A.B., Sousa Pereira, R.V., Marchesi, S.C., Alvarenga, D.M., Nakagaki, B.N., et al. (2016). Combination of mass cytometry and imaging analysis reveals origin, location, and functional repopulation of liver myeloid cells in mice. *Gastroenterology* 151, 1176–1191.
- Dill, B.D., Gierlinski, M., Hartlova, A., Arandilla, A.G., Guo, M., Clarke, R.G., and Trost, M. (2015). Quantitative proteome analysis of temporally resolved phagosomes following uptake via key phagocytic receptors. *Mol. Cell. Proteomics* 14, 1334–1349.
- Fairn, G.D., and Grinstein, S. (2012). How nascent phagosomes mature to become phagolysosomes. *Trends Immunol.* 33, 397–405.
- Flannagan, R.S., Cosio, G., and Grinstein, S. (2009). Antimicrobial mechanisms of phagocytes and bacterial evasion strategies. *Nat. Rev. Microbiol.* 7, 355–366.
- Flannagan, R.S., Heit, B., and Heinrichs, D.E. (2016). Intracellular replication of Staphylococcus aureus in mature phagolysosomes in macrophages precedes host cell death, and bacterial escape and dissemination. *Cell. Microbiol.* 18, 514–535.
- Flannagan, R.S., Kuiack, R.C., McGavin, M.J., and Heinrichs, D.E. (2018). Staphylococcus aureus uses the GraXRS regulatory system to sense and adapt to the acidified phagolysosome in macrophages. *MBio* 9, e01143–18.
- Gray, M.A., Choy, C.H., Dayam, R.M., Ospina-Escobar, E., Somerville, A., Xiao, X., Ferguson, S.M., and Botelho, R.J. (2016). Phagocytosis enhances lysosomal and bactericidal properties by activating the transcription factor TFEB. *Curr. Biol.* 26, 1955–1964.
- Hampton, M.B., Kettle, A.J., and Winterbourn, C.C. (1998). Inside the neutrophil phagosome: oxidants, myeloperoxidase, and bacterial killing. *Blood* 92, 3007–3017.
- Harrison, R.E., Bucci, C., Vieira, O.V., Schroer, T.A., and Grinstein, S. (2003). Phagosomes fuse with late endosomes and/or lysosomes by extension of membrane protrusions along microtubules: role of Rab7 and RILP. *Mol. Cell. Biol.* 23, 6494–6506.
- Horiuchi, H., Lippe, R., McBride, H.M., Rubino, M., Woodman, P., Stenmark, H., Rybin, V., Wilm, M., Ashman, K., Mann, M., et al. (1997). A novel Rab5 GDP/GTP exchange factor complexed to Rabaptin-5 links nucleotide exchange to effector recruitment and function. *Cell* 90, 1149–1159.
- Horn, J., Stelzner, K., Rudel, T., and Fraunholz, M. (2018). Inside job: Staphylococcus aureus host-pathogen interactions. *Int. J. Med. Microbiol.* 308, 607–624.
- Johnson, D.E., Ostrowski, P., Jaumouille, V., and Grinstein, S. (2016). The position of lysosomes within the cell determines their luminal pH. *J. Cell Biol.* 212, 677–692.
- Jubrail, J., Morris, P., Bewley, M.A., Stoneham, S., Johnston, S.A., Foster, S.J., Peden, A.A., Read, R.C., Marriott, H.M., and Dockrell, D.H. (2016). Inability to sustain intraphagolysosomal killing of Staphylococcus aureus predisposes to bacterial persistence in macrophages. *Cell. Microbiol.* 18, 80–96.
- King, J.S., Gueho, A., Hagedorn, M., Gopaldass, N., Leuba, F., Soldati, T., and Insall, R.H. (2013). WASH is required for lysosomal recycling and efficient autophagic and phagocytic digestion. *Mol. Biol. Cell* 24, 2714–2726.
- Li, H., Chan, L., Bartuzi, P., Melton, S.D., Weber, A., Ben-Shlomo, S., Varol, C., Raetz, M., Mao, X., Starokadomskyy, P., et al. (2014). Copper metabolism domain-containing 1 represses genes that promote inflammation and protects mice from colitis and colitis-associated cancer. *Gastroenterology* 147, 184–195.e3.
- Li, H., Koo, Y., Mao, X., Sifuentes-Dominguez, L., Morris, L.L., Jia, D., Miyata, N., Faulkner, R.A., van Deursen, J.M., Vooijs, M., et al. (2015). Endosomal sorting of Notch receptors through COMMD9-dependent pathways modulates Notch signaling. *J. Cell Biol.* 211, 605–617.
- Lippe, R., Miaczynska, M., Rybin, V., Runge, A., and Zerial, M. (2001). Functional synergy between Rab5 effector Rabaptin-5 and exchange factor Rabex-5 when physically associated in a complex. *Mol. Biol. Cell* 12, 2219–2228.
- Lorenzi, R., Brickell, P.M., Katz, D.R., Kinnon, C., and Thrasher, A.J. (2000). Wiskott-Aldrich syndrome protein is necessary for efficient IgG-mediated phagocytosis. *Blood* 95, 2943–2946.
- Lowy, F.D. (1998). Staphylococcus aureus infections. *N. Engl. J. Med.* 339, 520–532.
- Lukacs, G.L., Rotstein, O.D., and Grinstein, S. (1990). Phagosomal acidification is mediated by a vacuolar-type H(+)ATPase in murine macrophages. *J. Biol. Chem.* 265, 21099–21107.
- Magill, S.S., Edwards, J.R., and Fridkin, S.K.; Emerging Infections Program Healthcare-Associated Infections and Antimicrobial Use Prevalence Survey Team (2014). Survey of health care-associated infections. *N. Engl. J. Med.* 370, 2542–2543.
- Maine, G.N., Mao, X., Komarck, C.M., and Burstein, E. (2007). COMMD1 promotes the ubiquitination of NF-kappaB subunits through a cullin-containing ubiquitin ligase. *EMBO J.* 26, 436–447.
- Mouhadeb, O., Ben Shlomo, S., Cohen, K., Farkash, I., Gruber, S., Maharshak, N., Halpern, Z., Burstein, E., Gluck, N., and Varol, C. (2018). Impaired COMMD10-mediated regulation of Ly6C(hi) monocyte-driven inflammation disrupts Gut barrier function. *Front. Immunol.* 9, 2623.
- Muller, P.A., van de Sluis, B., Groot, A.J., Verbeek, D., Vonk, W.I., Maine, G.N., Burstein, E., Wijmenga, C., Vooijs, M., Reits, E., et al. (2009). Nuclear-cytosolic transport of COMMD1 regulates NF-kappaB and HIF-1 activity. *Traffic* 10, 514–527.
- Murata, K., Fang, C., Terao, C., Giannopoulou, E.G., Lee, Y.J., Lee, M.J., Mun, S.H., Bae, S., Qiao, Y., Yuan, R., et al. (2017). Hypoxia-sensitive COMMD1 integrates signaling and cellular metabolism in human macrophages and suppresses osteoclastogenesis. *Immunity* 47, 66–79.e5.
- Palmieri, M., Impey, S., Kang, H., di Ronza, A., Pelz, C., Sardiello, M., and Ballabio, A. (2011). Characterization of the CLEAR network reveals an integrated control of cellular clearance pathways. *Hum. Mol. Genet.* 20, 3852–3866.
- Panday, A., Sahoo, M.K., Osorio, D., and Batra, S. (2015). NADPH oxidases: an overview from structure to innate immunity-associated pathologies. *Cell. Mol. Immunol.* 12, 5–23.
- Phillips-Krawczak, C.A., Singla, A., Starokadomskyy, P., Deng, Z., Osborne, D.G., Li, H., Dick, C.J., Gomez, T.S., Koenecke, M., Zhang, J.S., et al. (2015). COMMD1 is linked to the WASH complex and regulates endosomal trafficking of the copper transporter ATP7A. *Mol. Biol. Cell* 26, 91–103.
- Pollitt, E.J.G., Szkuta, P.T., Burns, N., and Foster, S.J. (2018). Staphylococcus aureus infection dynamics. *PLoS Pathog.* 14, e1007112.
- Sardiello, M., Palmieri, M., di Ronza, A., Medina, D.L., Valenza, M., Gennarino, V.A., Di Malta, C., Donaudy, F., Embrione, V., Polishchuk, R.S., et al. (2009). A gene network regulating lysosomal biogenesis and function. *Science* 325, 473–477.
- Savina, A., Jancic, C., Hugues, S., Guernonprez, P., Vargas, P., Moura, I.C., Lennon-Dumenil, A.M., Seabra, M.C., Raposo, G., and Amigorena, S. (2006). NOX2 controls phagosomal pH to regulate antigen processing during crosspresentation by dendritic cells. *Cell* 126, 205–218.
- Segal, A.W., Geisow, M., Garcia, R., Harper, A., and Miller, R. (1981). The respiratory burst of phagocytic cells is associated with a rise in vacuolar pH. *Nature* 290, 406–409.
- Settembre, C., Di Malta, C., Polito, V.A., Garcia Arencibia, M., Vettrini, F., Erdin, S., Erdin, S.U., Huynh, T., Medina, D., Colella, P., et al. (2011). TFEB links autophagy to lysosomal biogenesis. *Science* 332, 1429–1433.
- Settembre, C., Fraldi, A., Medina, D.L., and Ballabio, A. (2013). Signals from the lysosome: a

control centre for cellular clearance and energy metabolism. *Nat. Rev. Mol. Cell Biol.* 14, 283–296.

Settembre, C., Zoncu, R., Medina, D.L., Vetrini, F., Erdin, S., Erdin, S., Huynh, T., Ferron, M., Karsenty, G., Vellard, M.C., et al. (2012). A lysosome-to-nucleus signalling mechanism senses and regulates the lysosome via mTOR and TFEB. *EMBO J.* 31, 1095–1108.

Sierro, F., Evrard, M., Rizzetto, S., Melino, M., Mitchell, A.J., Florido, M., Beattie, L., Walters, S.B., Tay, S.S., Lu, B., et al. (2017). A liver capsular network of monocyte-derived macrophages restricts hepatic dissemination of intraperitoneal bacteria by neutrophil recruitment. *Immunity* 47, 374–388.e6.

Starokadomskyy, P., Gluck, N., Li, H., Chen, B., Wallis, M., Maine, G.N., Mao, X., Zaidi, I.W., Hein, M.Y., McDonald, F.J., et al. (2013). CCDC22 deficiency in humans blunts activation of proinflammatory NF-kappaB signaling. *J. Clin. Invest.* 123, 2244–2256.

Strobel, M., Pfortner, H., Tuchscher, L., Volker, U., Schmidt, F., Kramko, N., Schnittler, H.J., Fraunholz, M.J., Löffler, B., Peters, G., et al. (2016). Post-invasion events after infection with *Staphylococcus aureus* are strongly dependent on both the host cell type and the infecting *S. aureus* strain. *Clin. Microbiol. Infect.* 22, 799–809.

Sturgill-Koszycki, S., Schaible, U.E., and Russell, D.G. (1996). Mycobacterium-containing

phagosomes are accessible to early endosomes and reflect a transitional state in normal phagosome biogenesis. *EMBO J.* 15, 6960–6968.

Surewaard, B.G., Deniset, J.F., Zemp, F.J., Amrein, M., Otto, M., Conly, J., Omri, A., Yates, R.M., and Kubes, P. (2016). Identification and treatment of the *Staphylococcus aureus* reservoir in vivo. *J. Exp. Med.* 213, 1141–1151.

Taylor, P.R., Martinez-Pomares, L., Stacey, M., Lin, H.H., Brown, G.D., and Gordon, S. (2005). Macrophage receptors and immune recognition. *Annu. Rev. Immunol.* 23, 901–944.

Thrasher, A.J., and Burns, S.O. (2010). WASP: a key immunological multitasker. *Nat. Rev. Immunol.* 10, 182–192.

Tsuboi, S., and Meerloo, J. (2007). Wiskott-Aldrich syndrome protein is a key regulator of the phagocytic cup formation in macrophages. *J. Biol. Chem.* 282, 34194–34203.

van de Sluis, B., Mao, X., Zhai, Y., Groot, A.J., Vermeulen, J.F., van der Wall, E., van Diest, P.J., Hofker, M.H., Wijnenga, C., Klomp, L.W., et al. (2010). COMMD1 disrupts HIF-1alpha/beta dimerization and inhibits human tumor cell invasion. *J. Clin. Invest.* 120, 2119–2130.

Varol, C., Mildner, A., and Jung, S. (2015). Macrophages: development and tissue specialization. *Annu. Rev. Immunol.* 33, 643–675.

Vieira, O.V., Bucci, C., Harrison, R.E., Trimble, W.S., Lanzetti, L., Gruenberg, J., Schreiber, A.D., Stahl, P.D., and Grinstein, S. (2003). Modulation of Rab5 and Rab7 recruitment to phagosomes by phosphatidylinositol 3-kinase. *Mol. Cell. Biol.* 23, 2501–2514.

Visvikis, O., Ihuegbu, N., Labed, S.A., Luhachack, L.G., Alves, A.F., Wollenberg, A.C., Stuart, L.M., Stormo, G.D., and Irazoqui, J.E. (2014). Innate host defense requires TFEB-mediated transcription of cytoprotective and antimicrobial genes. *Immunity* 40, 896–909.

Vural, A., Al-Khodori, S., Cheung, G.Y., Shi, C.S., Srinivasan, L., McQuiston, T.J., Hwang, I.Y., Yeh, A.J., Blumer, J.B., Briken, V., et al. (2016). Activator of G-protein signaling 3-induced lysosomal biogenesis limits macrophage intracellular bacterial infection. *J. Immunol.* 196, 846–856.

Yona, S., Kim, K.W., Wolf, Y., Mildner, A., Varol, D., Breker, M., Strauss-Ayali, D., Viukov, S., Guillemins, M., Misharin, A., et al. (2013). Fate mapping reveals origins and dynamics of monocytes and tissue macrophages under homeostasis. *Immunity* 38, 79–91.

Zigmond, E., Samia-Grinberg, S., Pasmanik-Chor, M., Brazowski, E., Shibolet, O., Halpern, Z., and Varol, C. (2014). Infiltrating monocyte-derived macrophages and resident kupffer cells display different ontogeny and functions in acute liver injury. *J. Immunol.* 193, 344–353.

ISCI, Volume 14

**Supplemental Information**

**COMMD10-Guided Phagolysosomal  
Maturation Promotes Clearance  
of *Staphylococcus aureus* in Macrophages**

**Shani Ben Shlomo, Odelia Mouhadeb, Keren Cohen, Chen Varol, and Nathan Gluck**

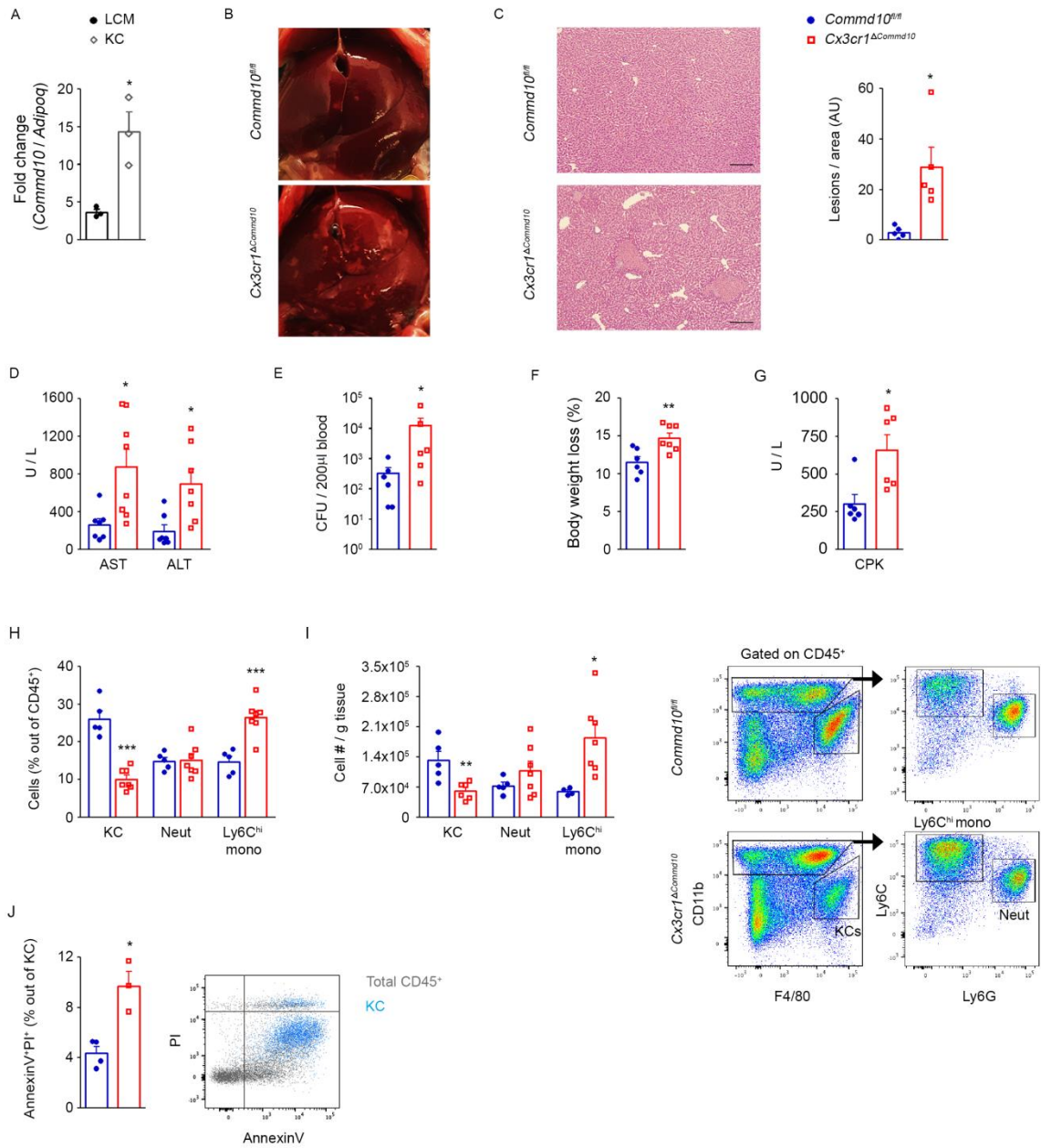


**Figure S1. Increased hepatic and systemic damage and KC death in *Cx3Cr1<sup>ΔCommd10</sup>* livers, Related to Figure 1.**

(A) *Commd10* gene expression in Liver capsular macrophages (LCM) and KC as extracted from existing databases of sorted KCs (GSE55606) and LCMs (E-MTAB-5932). *Commd10* expression was normalized to the expression of the adipocyte marker *Adipoq* (n=3). (B-J) *Commd10<sup>fl/fl</sup>* (blue closed circle) or *Cx3Cr1<sup>ΔCommd10</sup>* (red open square) mice were i.v. injected with *S. aureus* Rosenbach ( $5 \times 10^7$  CFU per animal) and sacrificed 24 h later. (B) Representative images of infected livers. Note the lesions appearing on the surface. (C) Left panel: representative images of Hematoxylin and eosin (H&E) staining of liver sections. Magnification x20, bar, 200  $\mu$ M. Right panel: quantification of lesions per liver area (AU, arbitrary units) (n=5). (D) Serum AST and ALT levels (Units/Liter) (n=8). (E) CFU per 200  $\mu$ l blood (n=8). (F) Body weight loss (n $\geq$ 6). (G) Serum CPK levels (Units/Liter) (n=6). (H) Assessment of KC, neutrophil and Ly6C<sup>hi</sup> monocyte fraction out of total CD45<sup>+</sup> immune cells (n $\geq$ 5). (I) Assessment of liver-resident KC, neutrophil and Ly6C<sup>hi</sup> monocyte numbers normalized to tissue mass (n $\geq$ 5). Right panel, representative flow cytometry images showing the gating strategy of KCs, neutrophils and Ly6C<sup>hi</sup> monocytes. (J) Assessment of AnnexinV<sup>+</sup>PI<sup>+</sup> KCs out of total population. Right panel, representative flow cytometry image showing AnnexinV<sup>+</sup>PI<sup>+</sup> KCs (light blue) over total CD45<sup>+</sup> immune cells (grey) (n $\geq$ 3). Data in A, E and J were analyzed by non-parametric Mann-Whitney test, and data in C, D, F-I were analyzed by unpaired two-tailed *t-test*, comparing each time between *Commd10<sup>fl/fl</sup>* and *Cx3cr1<sup>ΔCommd10</sup>* groups. Results are presented as mean  $\pm$  SEM with significance: \*p<0.05 \*\*p<0.01. \*\*\*p<0.001

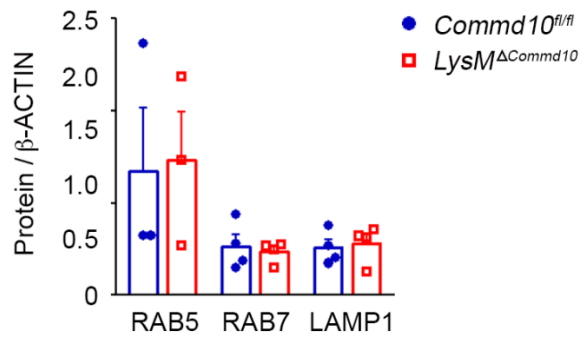


**Figure S2. Baseline expression of phagolysosomal maturation markers, Related to Figure 5.**

BMDM from *Commd1<sup>fl/fl</sup>* (blue closed circle) or *LysM<sup>ΔCommd10</sup>* (red open square) mice were lysed and analyzed by immunoblotting for protein expression of indicated phagolysosome maturation markers (n≥3). β-actin served as control. Densitometry graph is shown based on the zero time-point in immunoblot from Figure 5A. Data were analyzed by non-parametric Mann-Whitney test.

## **Transparent Methods**

### **Mice**

Animal experiments were performed with male adult C57BL/6J mice (8–12-wk old). Animals were maintained in specific pathogen-free animal facility and experiments were performed according to protocols and regulatory standards required by the Animal Care Use Committee of the Sourasky Medical Center (24-8-18). *LysM<sup>ΔCommD10</sup>* and *Cx3cr1<sup>ΔCommD10</sup>* mice were generated by crossing *Lyz2<sup>cre</sup>* and *Cx3cr1<sup>cre</sup>* (Yona et al., 2013) mice with *CommD10<sup>fl/fl</sup>* mice that were purchased from the EUCOMM consortium (strain EM:05951) (C57BL/6J background). Experiments with *LysM<sup>ΔCommD10</sup>* and *Cx3cr1<sup>ΔCommD10</sup>* mice were performed on mice heterozygous for these genes.

### **BMDM and neutrophil preparation**

BMDM were prepared by flushing BM from the femur and tibia and culturing in RPMI medium containing FBS (10%), penicillin (100 IU/ml), streptomycin (100 μg/ml) and macrophage-colony stimulating factor (M-CSF, 20 ng/ml), at 37°C in 5% CO<sub>2</sub>. Media was supplemented every 2-3 days. On day 6, macrophages were harvested and plated overnight at an assay-dependent concentration. Neutrophils were isolated using the neutrophil isolation kit (Miltenyi Biotec, Bergisch Gladbach, Germany cat# 130-092-332). Neutrophils were enriched to high purity (above 99%) and identified using flow cytometry as CD45<sup>+</sup>CD11b<sup>+</sup>CD115<sup>-</sup>Ly6G<sup>+</sup> cells.

### **Isolation of liver KCs**

Hepatic non-parenchymal cells were isolated by collagenase digestion buffer (0.5 mg/ml collagenase (C2139, Sigma), 5% Fetal bovine serum, PBS) followed by gradient centrifugation (Zigmond et al., 2014). KCs were enriched by selective adherence to plastic. Cells were seeded in DMEM containing 10% FBS, 1% L-Glutamine and 0.1% penicillin streptomycin, and incubated for 2 h in 5% CO<sub>2</sub> at 37°C. Non-adherent cells were then

removed by gently washing with PBS<sup>-/-</sup>. Cells were cultured for 7 days, (Gilboa et al., 2017). KC purity (88%) was determined by flow cytometry analysis. KCs were defined as CD45<sup>+</sup>CD11b<sup>int</sup>F4/80<sup>+</sup>CD64<sup>+</sup>Tim4<sup>+</sup>MHCII<sup>+</sup> cells.

#### Bacterial infection of KCs, BMDM and neutrophils

The following bacteria species were grown in LB broth at 37°C overnight: *S. xyloso*, *S. aureus Rosenbach* (clinical isolated ATCC-29213) and *SH1000-GFP S. aureus* (rsbU<sup>+</sup> NCTC8325-4 derivative (kindly provided by Dr. Ingo Schmitz, Helmholtz Center for Infection Research, Germany). Infection experiments were performed, unless indicated otherwise, at multiplicity of infection (MOI) = 5, with early log phase bacteria. At 30 min after infection, cells were washed and supplemented with gentamicin (100 ng/ml) to eliminate extracellular bacteria. At indicated times cells were washed twice with PBS<sup>-/-</sup> (without Ca<sup>++</sup> and Mg<sup>++</sup>), and collected for different analyses. The *SH1000-GFP S. aureus* were used in fluorescent assays; otherwise the *S. aureus Rosenbach* was used. With respect to TFEB, BMDM were infected with late log phase *S. aureus* at MOI=10.

#### Bacterial viability-colony forming unit assay

Tissues were weighed and homogenized (Polytron PT-MR 2100) in 1 ml PBS<sup>-/-</sup>. One million BMDM or KCs were homogenized in 0.1% triton x-100. Appropriate dilutions were seeded on LB agar plates and incubated at 37°C for 24 h. Isolated neutrophils (500,000/24 multiwell plate) were seeded in RPMI containing 10% FBS, 1% L-Glutamine and 0.1% penicillin streptomycin, and incubated for 30min in a 5% CO<sub>2</sub> at 37 °C. Non-adherent cells were removed by washing. Colonies were counted and presented as CFU per g tissue.

#### Protein immunoblotting

Total protein from one million BMDM was extracted in ice-cold RIPA buffer (C-9806S, Cell Signaling Tech. Beverly, Massachusetts) containing protease inhibitors (P8340, Sigma Aldrich St. Louis, Missouri). Proteins were detected by immunoblotting using standard

techniques. Antibodies used were: mTOR (2972), phosphorylated-mTOR ser2448 (2971) from Cell Signaling; GCN5 (sc-20698), RAB7 (sc-376362), RAB5 (sc-46692),  $\beta$ -ACTIN (sc-47778) from Santa Cruz; TFEB (A303-673A-T) from Bethyl Laboratories Inc; LAMP1 (ab24170), Cathepsin D [EPR3057Y] (ab75852) from Abcam; anti-COMMD10 antibody (GTX121488) from Genetex and RABAPTIN 5 (610676) from BD Biosciences, CCDC22 (16636-1-AP), CCDC93 (20861-1-AP) from ProteinTech Group, C16orf62 (PA5-28553) from Pierce. Blots were incubated with HRP-conjugated secondary antibodies, and subjected to chemiluminescent detection using the MicroChemi imaging system (DNR Bio-Imaging Systems, Israel). Densitometry was performed using ImageJ software. TFEB subcellular fractionation was performed using NE-PER nuclear/cytoplasmic extraction kit (78835, Thermo scientific, Paisley, UK) per manufacturer's instructions. Equivalent protein amounts were loaded for both nuclear and cytoplasmic fractions.

#### Confocal microscopy

BMDM and liver KCs were seeded (200,000/24 multiwell plate) overnight on cover glass. On the following day, cells were washed with medium and infected with *SH1000-GFP S. aureus* at MOI 20 for 1h. With respect to KCs, cells were infected at MOI 5 for 1h. Cells were then washed 3 times with PBS<sup>-/-</sup> and supplemented with 100 ng/ml gentamycin until indicated time points. Cells were fixed with 4% PFA for 10 minutes at 37°C. Slides were blocked and permeabilized with 0.1% saponin in blocking reagent (B10710, Thermofisher Scientific) for 45 min at room temperature, followed by overnight incubation at 4°C with specific antibodies for LAMP1 (ab24170) and COMMD10 (bs-8181R, Bioss, Woburn, Massachusetts). Slides were washed and then incubated for 1 h with the secondary antibody anti-rabbit Alexa Flour 647 (A31573, Life Technologies). Subsequently, slides were washed and mounted with fluorescent mounting medium without DAPI (E18-18, GBI labs, Bothell, Washington). For LysoTracker Red DND-99 (Invitrogen) staining, infected cells were

incubated with 50 nM dye for 30 min, washed with PBS, fixed with 2% PFA for 15 minutes and observed under the fluorescence microscope. Images were acquired using Zeiss LSM 700 confocal microscope with x100 (1.4 Oil DIC) and x40 (1.3 Oil DIC) oil objectives. Quantification of bacteria was performed utilizing ImageJ software on  $\geq 10$  separate fields (1 cell per field) for each group.

### Quantitative RT-PCR

Total RNA was extracted from *S. aureus* infected BMDM using the RNeasy Mini Kit (QIAGEN, Hilden, Germany). RNA was reverse transcribed with a high-capacity cDNA reverse transcription kit (Applied Biosystems, Foster City, California). All PCR reactions were performed with SYBR Green PCR Master Mix kit (Applied Biosystems) and Applied Biosystems 7300 Real-Time PCR machine. Quantification of PCR signals of each sample was performed by the  $\Delta C_t$  method normalized to *Gapdh*. Gene primers are listed in table:

	Forward	Reverse
<i>Acp5</i>	ATCATGTCTCTGGGGGACAA	AGAGACGTTGCCAAGGTGAT
<i>Commd1</i>	TGGCGAAGATGAGAGGACTT	GTGATGCCACCTTGCTTTTT
<i>Ccdc22</i>	CCTTGGAGCTTGGCTATCAG	AATGGCCCGAAGGAAAATAG
<i>Ccdc93</i>	GCAGCTGGCTATTTTCAGAGC	AAGAGCAAATCCACGTCCAC
<i>Commd10</i>	TGAGAAGTTCGCCAGAG	TTGCTCACTCCCAGTTGC
<i>Commd2</i>	CTC AAA GCT CAT GAT TTC	TGT CCA GAT AAA GCT GAA G
<i>Commd3</i>	TGA CAG AGA GCG AAT AGA AC	TGC CTA TAC TTC CCA GTA G
<i>Commd4</i>	CCA AGA TGT CCT CTG TGA AG	ACA TCG CCT GAC TCA AAC
<i>Commd5</i>	CTT TCA GAT GGG TCA GCA TAC	TTC AGA TAT CGC TTG AAG AGC
<i>Commd7</i>	GGC GCG CAG CAG TTC TCA	CGA TGC TTC TGA GGG AGC CAA G
<i>Commd8</i>	GTT TGG GAA TCA GAA GAA TG	GCT GAA ATA TCT CTT CAT CAG
<i>Commd9</i>	CCTCCTCTGACAACATCAGC	GGAGGGTTTCTCTCCACAC
<i>Ctsb</i>	AAATCAGGAGTATACAAGCATGA	GCCCAGGGATGCGGATGG
<i>Ctsd</i>	CTGAGTGGCTTCATGGGAAT	CCTGACAGTGGAGAAGGAGC
<i>Ctsk</i>	ATGTGAACCATGCAGTGTGGTGG	ATGCCGCAGGCGTTGTTCTTATTC
<i>Gapdh</i>	TGCAGTGGCAAAGTGGAGAT	TGCCGTGAGTGGAGTCATACT
<i>Il1b</i>	GCTGAAAGCTCTCCACCTCA	AGGCCACAGGTATTTTGTCTG
<i>Il6</i>	GTTCTCTGGGAAATCGTGGA	TTTCTGCAAGTGCATCATCG
<i>Lamp1</i>	AGGCCACTGTGGAAACTCATACA	TTCCACAGACCCAAACCTGTCACT
<i>Lamp2</i>	ATTGGGGTATTACCTGCAA	TTGGAGTTGGAGTGGGTGTT
<i>Lipa</i>	CACCTGGTCTCTGAAGCACA	GCCTTGAGAATGACCCACAT
<i>Scarb2</i>	GGTGTGTCTTTGGCTTGGT	TAGGTTCTGATAGGGGGTGC
<i>Nox2</i>	CCCTTTGGTACAGCCAGTGAAGAT	CAATCCCAGCTCCCCTAACTCA

## ELISA

Supernatants from BMDM were collected. The level of IL-1 $\beta$  was assessed with the DuoSet ELISA kit (R&D Systems).

## Flow cytometry analysis

The following anti-mouse antibodies were used (dilutions are indicated): CD45 (clone 30-F11, 1:100), CD11b (clone M1/70, 1:300), CD64 (clone X54-5/7.1, 1:50), TIM4 (clone RMT4-54, 1:50), all purchased from BioLegend, San Diego, USA. Anti-mouse F4/80 (clone A3-1, 1:50) was purchased from BIORAD. The staining for ROS was performed with 0.1 mM of 2,7-dichlorodihydrofluoresceindiacetate (Molecular Probes Invitrogen). Staining for apoptosis and necrosis markers with Annexin V and propidium iodide (PI) was performed with MEBCYTO-Apoptosis Kit (MBL International Corporation). Cells were analyzed with BD FACSCanto™ II (BD Bioscience). Flow cytometry analysis was performed using FlowJo software (TreeStar, Ashland, OR, USA).

## Staining of bacteria with pHrodo

*S. aureus Rosenbach* were incubated with 10 $\mu$ M pHrodo (P36600, Life Technology) in the dark at 37°C, with shaking (250 rpm) for 30 min. Bacteria were centrifuged at 9300g for 1 min and the pellet was washed and resuspended in PBS<sup>-/-</sup> (Jubrail et al., 2016). BMDM were infected with the pHrodo-tagged bacteria as mentioned above and fixed in 0.2% PFA for 30 min at RT. About 80 macrophages were counted and the number of pHrodo bright/dim bacteria per macrophage was counted. Images were acquired using the confocal microscope (1.4 oil DIC lens). Additionally, pHrodo fluorescence intensity in infected macrophages was measured by a fluorescent plate reader.

## Measurement of intracellular ROS

BMDM were infected with *S. aureus* (MOI=5). At indicated times, cells were washed with PBS<sup>-/-</sup> and incubated with 20µM 2',7'-dichlorofluorescein diacetate (DCFH-DA) (D6883, Sigma Aldrich) for 30min at 37°C. Cells were analyzed by flow cytometry.

#### Cathepsin D activity measurement

BMDM were infected with *S. aureus* (MOI=5) as described above for 2 h. Cathepsin D activity (fluorescence released by cleavage, HiLyte Fluor<sup>TM</sup> 488) was measured by fluorescence microplate reader using Sensolyte 520 Cathepsin D assay kit (AS-72170, Anaspec EGT Group, Fremont, CA).

#### Internalization of *S. aureus* bioparticles

*S. aureus* internalization into BMDM was assessed by using opsonized *S. aureus* bioparticles. Briefly, *S. aureus*, Wood strain without protein A (S-2851, Molecular probes), were opsonized with bioparticles opsonizing reagent (S-2860, Molecular probes) at a 1:1 ratio for 1 h at 37°C, followed by 3 washes with PBS<sup>-/-</sup>. Bioparticles were added to BMDM at MOI=50 for 3 h. Cells were washed, detached, and fluorescence intensity was analyzed by flow cytometry. Additionally, 500,000 BMDM were seeded in bottom glass cell culture dish and challenged as described above. Internalization was imaged by confocal microscopy (1.3 Oil DIC lens). Cells with 10 or more bacteria bioparticles were imaged.

#### *In vivo S. aureus* infection model

Mice were injected with early log phase *S. aureus*, 5x10<sup>7</sup> CFU, in 200µl saline via the tail vein. Mice were sacrificed at indicated time points and liver and blood were collected for different analyses.

#### Gene-expression data mining

Gene expression of *Commd10* and *Adipoq* was extracted out of existing databases of sorted steady state KCs (Zigmond et al., 2014) and LCMs (Sierro et al., 2017), deposited at the

National Center for Biotechnology Information Gene Expression Omnibus public database2 (GSE55606) and ArrayExpress database (E-MTAB-5932), respectively.

#### Quantification of hepatic damage

Liver samples were obtained at 24 h after *S. aureus* infection, fixed (4% para-formaldehyde), paraffin-embedded, sectioned, and stained with H&E. Pathologic evaluation was performed by an expert pathologist. The number of necrotic lesions was calculated and normalized to sample area as measured by ImageJ software in scanned slides. Serum alanine aminotransferase (ALT) and aspartate aminotransferase (AST) levels were measured using a Hitachi 747 Automatic Analyzer.

#### Statistical analysis

Statistical differences between two groups were determined accordingly: in cases where samples distributed normally according to Kolmogorov-Smirnov Test we used unpaired two-tailed t-test with GraphPad. When the sample did not distribute normally, we used Mann Whitney Test with GraphPad. Statistical differences between three groups were determined using one way ANOVA with Tukey post-tests using Graphpad. Significance was defined if p-value was less than 0.05 as following: \*  $p < 0.05$ ; \*\*  $p < 0.01$ ; \*\*\*  $p < 0.001$ .